Published in final edited form as:
Neurobiol Dis. 2014 October ; 70: 74–89. doi:10.1016/j.nbd.2014.06.004.

The prostaglandin EP1 receptor potentiates kainate receptor activation via a protein kinase C pathway and exacerbates status epilepticus

Asheebo Rojas, **Paoula Gueorguieva**, **Nadia Lelutiu**, **Yi Quan**, **Renee Shaw**, and **Raymond Dingledine**
Department of Pharmacology, Emory University, 1510 Clifton Road NE, Atlanta, GA 30322

Abstract

Prostaglandin E2 (PGE2) regulates membrane excitability, synaptic transmission, plasticity, and neuronal survival. The consequences of PGE2 release following seizures has been the subject of much study. Here we demonstrate that the prostaglandin E2 receptor 1 (EP1, or *Ptger1*) modulates native kainate receptors, a family of ionotropic glutamate receptors widely expressed throughout the central nervous system. Global ablation of the EP1 gene in mice (EP1-KO) had no effect on seizure threshold after kainate injection but reduced the likelihood to enter status epilepticus. EP1-KO mice that did experience typical status epilepticus had reduced hippocampal neurodegeneration and a blunted inflammatory response. Further studies with native prostanoid and kainate receptors in cultured cortical neurons, as well as with recombinant prostanoid and kainate receptors expressed in *Xenopus* oocytes, demonstrated that EP1 receptor activation potentiates heteromeric but not homomeric kainate receptors via a second messenger cascade involving phospholipase C, calcium and protein kinase C. Three critical GluK5 C-terminal serines underlie the potentiation of the GluK2/GluK5 receptor by EP1 activation. Taken together, these results indicate that EP1 receptor activation during seizures, through a protein kinase C pathway, increases the probability of kainic acid induced status epilepticus, and independently promotes hippocampal neurodegeneration and a broad inflammatory response.

Keywords

EP1; EP2; GluK2; GluK4; GluK5; Kainate receptor; AMPA; Protein Kinase C; status epilepticus

Correspondence to: Asheebo Rojas, PhD Department of Pharmacology Emory University School of Medicine Atlanta, GA 30322 Phone: 404-727-5635 Fax: 404-727-0365 arojas@pharm.emory.edu.

Participated in research design: Rojas and Dingledine.
Conducted experiments: Rojas, Gueorguieva, Quan, Lelutiu and Shaw.
Performed data analysis: Rojas, Gueorguieva, Quan and Dingledine.
Wrote or contributed to the writing of the manuscript: Rojas and Dingledine

INTRODUCTION

PGE2, a major cyclooxygenase 2 product in the mammalian brain, exerts hormone-like properties that modulate many physiological and pathophysiological functions, among them membrane excitability and synaptic transmission in CA1 pyramidal neurons (Chen and Bazan, 2005). However, the pathways and mechanisms involved remain largely unknown. Kainic acid, an excitatory neurotoxin, when injected into rodents at doses ≥ 20 mg/kg induces seizures that can progress into status epilepticus, which in turn eventually causes development of spontaneous recurrent seizures (epilepsy) in the weeks following (Ben-Ari et al., 1979; Hellier et al., 1998). Kainate receptors (KARs) are ionotropic glutamate receptors composed of GluK1 through GluK5 subunits that are located both presynaptically and postsynaptically throughout the CNS and are involved in synaptic plasticity and transmission (Kamiya, 2002; Huettner, 2003; Lerma, 2003; Pinheiro and Mulle, 2006). Recently we demonstrated expression of the high affinity kainate receptor subunits (GluK4 and GluK5) in the CA3 region of the hippocampus (Rojas et al., 2013), which supported a previous report by Darstein et al. (2003). The expression profile of the high affinity kainate receptor subunits is consistent with the localization of kainic acid binding in the hippocampus. Furthermore, the expression profile of GluK5 (one of the high affinity KA subunits) correlates with the neurodegeneration pattern in the hippocampus following kainic acid injection in rodents.

A prominent neuropathology associated with kainic acid induced status epilepticus is hippocampal neurodegeneration. Recent studies have suggested that signaling via the prostaglandin EP1 receptor may affect the fate of neurons following brain injury. For example, EP1 deficient mice show less neuronal injury following transient forebrain ischemia (Shimamura et al., 2013) and cerebral ischemia (Zhen et al., 2012). Pharmacological inhibition of the EP1 receptor with SC51089 reduces neuronal loss and blood-brain barrier disruption following ischemic injury (Shimamura et al., 2013; Fukumoto et al., 2010) suggesting that EP1 activation may promote cell death. Kawano et al. (2006) demonstrated that EP1 gene inactivation reduced brain injury following NMDA induced excitotoxicity, ischemia or oxygen glucose deprivation, suggesting that the presence of EP1 in normal animals contributes to or exacerbates the injury. Each glutamate receptor subtype (NMDA, AMPA and KA) is likely to play a role in the above mentioned brain injury models. Endogenous kainate receptors are regulated by $G_{\alpha q}$ coupled receptors that are known to modulate excitotoxicity following seizures (Benveniste et al., 2010; Rojas et al., 2013). EP1 is a $G_{\alpha q}$-coupled receptor for PGE2, thus we hypothesized that kainate receptors are targeted by EP1 pathways to contribute to the neuropathology that follows status epilepticus. Here we ask the questions: Does genetic inactivation of EP1 alter kainate induced status epilepticus? Do EP1 knockout mice display reduced neurodegeneration or brain inflammation following kainate induced status epilepticus? Is there cross-talk between kainate receptors and prostanoid receptors and if so, what is the mechanism? To address these questions we combined an *in vivo* rodent model of kainate induced status epilepticus and functional *in vitro* studies of native and co-expressed recombinant kainate receptors and prostanoid receptors.

MATERIALS AND METHODS

Kainic acid injection

All procedures and experiments conformed to the guidelines of the Animal Care and Use Committee of Emory University. Every effort was made to minimize animal suffering. Wildtype (WT) adult male C57BL/6 mice (≥20 g) were obtained from Charles Rivers Labs (Wilmington, MA, USA). EP1 knockout mice (EP1-KO) (Ptger1^{tm1Dgen}; stock number 011638) were purchased from the Mutant Mouse Regional Resources Center (MMRRC) through the Jackson Laboratory. Disruption of the EP1 gene had been produced by targeted insertion of the LacZ gene that drives β-galactosidase activity. The EP1-KO mice display reduced blood pressure and impulsive behavior (Guan et al., 2007; Stock et al., 2001; Matsuoka et al., 2005). Otherwise, they appear normal and their brains develop normally. The Jackson Laboratory C57BL/6 mice show a higher mortality than the Charles Rivers Laboratories C57BL/6 mice during status epilepticus (Borges et al., 2003) and thus the EP1-KO mice were bred for six to eight generations from the C57BL/6 Jackson Laboratory strain into the C57BL/6 Charles River Laboratories strain to generate homozygous knockouts. Mice were housed under a 12 hour light/dark cycle with food and water *ad libidum*. Total RNA was isolated from half brains of wildtype and EP1-KO mice injected with kainate four days prior to verify disruption of the EP1 gene by a targeted insert of the LacZ gene. The presence of a 584 bp amplicon that represents the LacZ targeted gene insertion used to disrupt the EP1 gene suggests functional EP1 disruption in the 14 brains taken from EP1-KO mice that experienced status epilepticus. End point PCR was performed on the samples using two sets of primers; one set to identify wildtype (a 272 bp amplicon) and the other set to identify the EP1 disrupted gene (a 584 bp amplicon). The primer sequences are as follows: wildtype forward: 5’-CCAACAGGCGATAATGGCACATCAC-3’; EP1-KO (target insertion) forward: 5'-GGGGATCGATCCGTCCTGTAAGTCT-3'; and a common reverse: 5’-ACCATGCAGCCACCCAGGAAATGAC-3’ for both. The PCR products were separated on a 1% ethidium bromide agarose gel and imaged under UV. In a separate experiment total RNA was also isolated from the hippocampi of 8 untreated male wild-type C57BL/6 mice to verify expression of the EP1 gene. End point PCR was performed using the wildtype primer set as described above. We could not use immunohistochemistry to verify loss of the EP1 receptor because three different antibodies showed the same pattern of hippocampal pyramidal cell labeling in sections obtained from wildtype mice and EP1-KO mice prepared by two different strategies.

Kainate was obtained from Tocris Bioscience (Ellisville, MO) and was dissolved at 4 mg/ml in a physiological (0.9%) saline (pH 7.4) to generate a stock solution. The stock solution was diluted in 0.9% saline to create fresh working solutions on the injection day. Mice were weighed and injected with a single dose of kainate (5, 10, 20, 30 or 40 mg/kg) subcutaneously (s.c.) at 10 ml/kg. Subcutaneous injection was chosen as the route of administration for the single dose exposure to eliminate any complications from the injection (e.g. injecting into an internal organ). Control mice received 0.9% saline instead of kainate. Additional groups of wildtype and EP1-KO mice were injected with only a high dose of kainic acid (30 or 40 mg/kg) intraperitoneally (i.p.) to obtain a high enough proportion of mice who survive after status epilepticus; if the mice did not enter status

epilepticus within 30 min they received another dose of 10 mg/kg. In mice, kainate-induced seizures consisted of distinct motor behaviors, including forelimb clonus, loss of posture, rearing, and falling. Animals presenting these behaviors with increased seizure intensity, duration, and frequency shortly after the injection of kainate were declared to be in status epilepticus, which is characterized in the kainate model by periodic rearing and falling accompanied by whole body clonic seizures. Behavior was scored using a modified Racine scale (Racine, 1972) shown below. All mice that entered status epilepticus continued seizing for at least 90 minutes; seizures usually persisted for several hours and eventually waned and stopped. To increase survival of animals, hyperthermia was minimized during status epilepticus by periodic cooling of the animals with chilled air. Following status epilepticus the mice were hydrated with lactate ringers and allowed to recover overnight.

Behavioral Score	Observed Motor Behavior
0 **Normal Behavior:**	walking, exploring, sniffing, grooming
1 **Freeze Behavior:**	immobile, staring, heightened startle, curled-up posture
2 **Automatisms:**	blinking, head bobbing, scratching, face washing, whisker twitching, chewing, star gazing
3 **Early Seizure Behavior:**	myoclonic jerks, partial or whole body clonus (flexions and extensions of body muscles)
4 **Advance Seizure Behavior:**	rearing and falling, loss of posture (e.g. falling, corkscrew turning, splaying of limbs)
5. **Status Epilepticus:**	repeated seizure activity (≥2 events in stages 3, 4 or 6 within a 5 minute window), which lasts ≥ 30 min
6 **Intense Seizure Behavior:**	repetitive jumping or bouncing, wild running, tonic seizures
7 **Death**	

A behavior score was assigned to an animal when it exhibited at least two different signs within that score group during a 5 min observation period.

FluoroJade labeling

Four days after status epilepticus onset, wildtype and EP1-KO mice along with the saline controls were anesthetized deeply with isoflurane. The mice were decapitated and their brains were rapidly removed and longitudinally bisected. One-half of the brain was fixed overnight in a 4% paraformaldehyde solution at 4°C. The other half excluding the cerebellum and hind brain was frozen on dry ice and kept for RNA isolation. The next day the half brains post-fixed in 4% paraformaldehyde were transferred to 30% (w/v) sucrose in phosphate buffered saline at 4°C until they sank. Fixed mouse half brains were dehydrated, embedded in paraffin and sectioned (8 μm) coronally through the hippocampus and mounted onto slides. Every 20th hippocampal section was labeled with cresyl violet. Every 5th section excluding those used for cresyl violet for a total of ~40 sections from each half mouse brain was used for FluoroJade staining to label degenerating cells according to the manufacturer protocol (Histo-chem Inc., Jefferson, AR) as described by Schmued et al. (1997). Briefly, slides were immersed in 100% ethyl alcohol for 3 min followed by a 1 min immersion in 70% alcohol and a 1 min immersion in distilled water. The slides were then transferred to a solution of 0.06% potassium permanganate for 15 min and were gently shaken on a rotating platform at 25 °C. The sections were rinsed for 1 min in distilled water and then transferred

to the 0.001% FluoroJade B staining solution where they were gently agitated for 30 min. Following staining, the sections were rinsed with three 1 min washes of 1× Tris buffered solution (TBS) and allowed to dry. The sections were made transparent with xylenes and mounted under D.P.X. (Electron Microscopy Sciences, Hatfield, PA) mounting medium. FluoroJade labeling was visualized using an Axio Observer A1 epifluorescence microscope equipped with an AxioCam MRc 5 camera and a filter suitable for visualizing fluorescein or FITC (Zeiss, Oberkochen, Germany). Images were taken using AxioVision AC 4.7 software (Zeiss).

Following FluoroJade B staining, images were obtained from three hippocampal areas (hilus, CA1, CA3) at 50× magnification. The number of bright FluoroJade B positive neurons in the hippocampus was counted by another researcher unaware of the experimental conditions. Only FluoroJade B positive cells with a near complete cell body shape and size when compared to normal healthy pyramidal neurons stained with cresyl violet were counted from ~40 sections per mouse through the majority of the hippocampus from rostral (Bregma -1.34 mm) to caudal (Bregma -3.4 mm) based on the mouse brain atlas. Cell counts were expressed as the total number of FluoroJade B positive cells per section. This approach was used because the staining was patchy throughout the hippocampus.

RNA isolation and quantitative real-time polymerase chain reaction (qRT-PCR)

Total RNA was isolated using Trizol with the PureLink RNA Mini Kit (Invitrogen) from the frozen half brains of mice that experienced status epilepticus and were sacrificed 24 hours or four days later. RNA concentration and purity were measured by a spectrophotometer using the A260 value and the A260/A280 ratio, respectively. First-strand cDNA synthesis was performed with 0.2 μg of total RNA, 200 units of SuperScript II Reverse Transcriptase (Invitrogen), and 0.5 μg random primers in a reaction volume of 30 μl at 42 °C for 50 minutes. The reaction was terminated by heating at 70 °C for 15 minutes. qRT-PCR was performed by using 8 μl of 10× diluted cDNA, 0.1–0.5 μM of primers, and 2× iQ SYBR Green Supermix (Bio-Rad Laboratories) with a final volume of 20 μl in the iQ5 Multicolor Real-Time PCR Detection System (Bio-Rad Laboratories). Cycling conditions were as follows: 95 °C for 2 minutes followed by 40 cycles of 95 °C for 15 seconds and 60 °C for 1 minute. Melting curve analysis was used to verify single-species PCR product. Fluorescent data were acquired at the 60 °C step. The geometric mean of cycle thresholds for β-actin, GAPDH, and HPRT1 was used as an internal control for relative quantification. Table 1 demonstrates that the mean CT values of these housekeeping genes and the geometric means are similar in all four groups of animals that were sacrificed 24 hours after status epilepticus. Samples without cDNA template served as the negative controls.

Cortical cell culture

The entire cortex was isolated from embryonic-day 16 to 18 embryos of either timed-pregnant Sprague-Dawley rats or wildtype C57BL/6 or EP1-KO mice. The tissue was dissociated following papain exposure and the cells were plated as described by Jiang et al. (2010). Both neuron dense and astrocyte dense cultures were prepared at the same time. Briefly, after dissociation the cells intended for neuron dense cultures were counted and plated onto poly-D-lysine coated 96-well plates (black with clear bottom) at a density of

150,000 cells/well for rat cultures and 100,000 cells/well for mouse cultures in Neurobasal medium supplemented with B27 and 5% FBS (Invitrogen, Carlsbad, CA). Calcium assay experiments were performed after 5-10 DIV. Cells from the neuron dense cultures were also plated onto poly-D-lysine coated coverslips in 24-well tissue culture plates in Neurobasal medium supplemented with B27 and 5% FBS for immunocytochemistry experiments at 7 DIV. For astrocyte dense cultures isolated embryonic rat pup cortices were dissociated without enzyme digestion and were initially incubated in T-75 flasks in MEM supplemented with 10% FBS for 10 DIV. The neurons were removed from the astrocyte cultures in two steps. First, the plates were shaken on DIV 11 to displace the neurons and they were removed by replacing the media. Secondly, the cultures were trypsinized and the astrocytes were re-plated onto poly-D-lysine-coated 96-well plates for calcium assay experiments or poly-D-lysine coated coverslips for immunocytochemistry in MEM supplemented with 10% FBS on DIV 14 to favor neuron death and astrocyte growth. Cultures were incubated at 37 °C in 95% air/5% CO_2 and half of the culture medium was replaced every 3 to 4 days with serum-free medium for neuron dense cultures and medium containing 10% FBS for astrocyte cultures.

Immunocytochemistry

Neuron dense and astrocyte dense cultures prepared from rat embryos were fixed with 4% paraformaldehyde for 10 minutes and were washed three times with 1× PBS, blocked for 2 hours in PBS containing 1% BSA and incubated overnight in the primary antibody mouse anti-glial fibrillary acidic protein (mouse anti-GFAP, Santa Cruz Biotechnology), rabbit anti-microtubule associated protein 2 (rabbit anti-MAP2, Millipore), mouse anti-ionized calcium-binding adapter molecule 1 (mouse anti-Iba1, Santa Cruz Biotechnology) or rabbit anti- cluster of differentiation 31 (rabbit anti-CD31, Abcam) each diluted at 1:2000. All antisera dilutions were done in a PBS based antibody dilution solution (ADS) containing 0.1% gelatin, 0.1% sodium azide and 0.25% Triton X-100. After washing three times with ADS the cells were incubated with the appropriate Alexa Fluor fluorophore-conjugated secondary antibody (Alexa Fluor goat anti-rabbit 488 or goat anti-mouse 546, Molecular Probes, Eugene, OR) diluted to 1:500 in ADS for 4 hrs at 25 °C. The cells were washed three times with PBS and then incubated with the blue-fluorescent Hoechst 33342 dye (Molecular Probes, Eugene, OR) diluted 1:5000 in ADS for 4 hrs at 25 °C. The cells were again washed with PBS and mounted with FluoroGel mount. Fluorescence images were acquired using an Olympus BX51WI spinning disk (high speed) confocal microscope (Center Valley, PA), using Slide book 4.2 software (Intelligent Imaging Innovations, Denver, CO). In control experiments, the cells were treated in a similar manner except the primary antibodies were omitted. All negative controls showed no staining (data not shown).

Immunohistochemistry

All experimental procedures were performed in accordance with the guidelines for the Care and Use of Laboratory Animals by Emory University. For GFAP immunohistochemistry twelve male C57BL/6 mice (≥20 g) from Charles Rivers Laboratories and nine EP1-KO (≥20 g) mice that experienced status epilepticus four days earlier were deeply anesthetized by inhalation with isoflurane and decapitated. The brains were rapidly dissected and bisected longitudinally. The half-brains were post-fixed in 4% (wt/vol) paraformaldehyde in 0.1 M

phosphate-buffered saline (PBS; pH, 7.4) at 4°C overnight, and then transferred to 30% (w/v) sucrose in phosphate buffer at 4°C until they sank. The half-brains were then embedded in paraffin and coronal sections (8 μm) were cut throughout the hippocampus using a sliding microtome and mounted on slides. The sections were then dewaxed and used for fluorescence immunohistochemistry. The sections were washed three times with 1X PBS, blocked for 45 minutes in PBS containing 1% BSA, and incubated in the primary antibody (rabbit anti-GFAP, 1:1000; Dako, Carpinteria, CA) diluted in ADS containing 0.1% gelatin and 0.3% Triton X-100 in PBS at 4°C for 24 hours. After washing three times with ADS, the sections were incubated with an Alexa Fluor fluorophore-conjugated secondary antibody (AlexaFluor goat anti-rabbit 488 (1:1000) for GFAP; Molecular Probes, Eugene, OR) diluted in ADS for 4 hours at 25°C. The sections were again washed with PBS, mounted onto slides, allowed to dry, and finalized by the addition of Fluoro Gel mounting media and a cover slip. The fluorescence reactions were visualized using an Axio Observer A1 flourescence microscope (Zeiss, Oberkochen, Germany). Pictures were taken using the AxioVision AC 4.1 software (Zeiss). In control experiments, the sections were treated in a similar manner, except that the primary antibodies were omitted. All negative control sections showed no staining (data not shown). Quantification of GFAP immunohistochemistry was carried out using Pixcavator IA 6.0 (Intelligent Perception, Huntington, WV). The GFAP positive images (200× total magnification) taken from the CA3 region of three dorsal hippocampal sections obtained from the brains of wildtype (n=12) and EP1-KO (n=9) mice that experienced status epilepticus 4 days earlier were uploaded into Pixcavator and the roundness of the astrocytes was measured using the equation:

$$roundness=4\pi\left(\frac{area}{perimeter^2}\right)\times 100$$

Measurement of $[Ca^{2+}]_i$ in cortical cultures

Cortical neurons and glia from pups of rats or mice were prepared in 96-well plates as described above. After 5 days *in vitro* (neuron dense cultures) or 20 days *in vitro* (astrocyte dense cultures) the level of intracellular calcium in the cultures was assayed using the Fluo-4 no wash calcium assay kit according to the manufacturer's protocol (Invitrogen, Carlsbad, CA). Briefly, the culture media was removed and replaced with a calcium assay buffer (CAB) containing 1x HBSS, 20 mM HEPES, 2.5 mM Probenacid, and Fluo4-NW dye mix, pH 7.4 (Invitrogen, Carlsbad, CA). The cells were then incubated for 45 minutes at 37 °C for dye loading and then 15 minutes at 25 °C. To isolate calcium signals mediated by heteromeric kainate receptors, we used AMPA, kainate and domoate as agonists and added a cocktail of NMDA, GABA and AMPA receptor antagonists (10 μM MK801, 100 μM D-AP5, 100 μM Bicuculline, and 100 μM GYKI52466) to the CAB prior to dye loading. The calcium fluorescence measurement was performed at 25 °C. CAB with or without PGE2 or 17-PT (25 μl, 5X final concentration) was added after 60 seconds of baseline recording with a FLEXstation II benchtop scanning fluorometer (Molecular Devices, Eugene, OR), then a glutamate receptor agonist (25 μl, 6X) was added at 180 seconds. Fluorescence plate reading continued for a total of 400 seconds using an excitation wavelength of 485 nm, an emission

of 538 nm, and a cutoff of 530 nm. Agonist and vehicle were added at a speed of 26 μl/second. The data were recorded using SoftMax Pro software (Molecular Devices, Eugene, OR). The calcium data were expressed as "fluorescent counts" which is defined as relative fluorescent units (RFU) with baseline correction (first 60 seconds of the recording).

Molecular biology

Rat GluK2(R) (GenBank #NM_019309.2) in the pSGEM vector was a generous gift from Dr. Mark Mayer (National Institutes of Health, Bethesda, MD). Plasmids encoding rat GluK1 (GenBank #NM_001111117.1), GluK4 (GenBank # U08257) and GluK5 (GenBank #NM_031508) were generously provided by Dr. Stephen Heinemann (Salk Institute, San Diego, CA). Human EP1 (GenBank #AY275470) and EP2 (GenBank # AY275471) cDNA were purchased from the University of Missouri-Rolla cDNA resource center (EP1, #PER0100000; EP2, #PER0200000). Both EP1 and EP2 were subcloned into the RNA vector pSGEM. GluK5 mutations were generated using the QuikChange site-directed mutagenesis kit (Stratagene, La Jolla, CA) according to the manufacturer's protocol. All mutants were subcloned back into the original receptor vector (i.e. pGEM, pSGEM, or pCMVTNT for GluK5) using the SphI and XbaI sites. Correct constructions and mutations were confirmed by DNA sequencing. All cRNAs were transcribed *in vitro* from linearized cDNA templates utilizing the mMessage mMachine kit (Ambion, Austin, TX) and purified for injection into oocytes.

Oocyte preparation and recording

All procedures and experiments conformed to the guidelines of the Animal Care and Use Committee of Emory University. *Xenopus* oocytes were prepared and injected as described previously (Curras and Dingledine, 1992). Briefly, Stage V-VI oocytes were removed from frogs that had been anesthetized in water containing 0.156% tricaine. After treatment with type IV collagenase (Worthington Biochemical, Lakewood, NJ; 1.7 mg/ml for 45–120 min) in a calcium-free Barth's solution, oocytes rested overnight and were then injected with 50-100 ng of mRNA transcribed from linearized constructs in the pCMVTNT, pSGEM, or pBluescript vectors. For the expression of heteromeric receptors mRNAs were injected at a 1:3 weight ratio (GluK2/GluK4 and GluK2/GluK5) with or without an equal weight of EP1 or EP2 mRNA. Before electrophysiological recording, injected oocytes were maintained at 18 ^{o}C for 3-10 days in Barth's solution containing (in mM) NaCl 88, $NaHCO_3$ 2.4, KCl 1, $Ca(NO_3)_2$ 0.33, $CaCl_2$ 0.91, $MgSO_4$ 0.82, Tris/HCl 5, (pH = 7.4) and supplemented with gentamycin (100 μg/ml), penicillin (10 U/ml) and streptomycin (10 μg/ml).

Two-electrode voltage-clamp recordings were performed at room temperature (23-25 °C) from cells continually perfused in a standard frog Ringer's solution containing (in mM): 90 NaCl, 1 KCl, 15 HEPES, and 0.5 $BaCl_2$ (pH 7.4). Recording pipettes were filled with 3 M KCl. GluK2 homomeric receptors were activated by bath application of domoate (3 μM). GluK2/GluK4 and GluK2/GluK5 receptors were activated by bath application of AMPA (1-300 μM). Currents were elicited from a holding potential of −60 mV unless otherwise specified. Currents were digitized at 1 kHz with a Digidata 1200 analog to digital converter (Axon Instruments, Foster City, CA) under the control of pClamp 8 acquisition software (Molecular Devices, Sunnyvale, CA) and stored on a computer disk for later analysis.

Application of each agonist produced in the majority of oocytes a rapidly rising current that reached steady state. Results from oocytes in which the agonist-induced current was not stable under baseline conditions, or the baseline holding current at the beginning and end of the experiment drifted by more than 10%, were discarded.

Chemicals and reagents

(2*S*,3*S*,4*S*)-Carboxy-4-(1-methylethenyl)-3-pyrrolidineacetic acid (kainic acid), (2*S*,3*S*,4*R*,5'*R*)-2-Carboxy-4-(5'-carboxy-1'-methyl-1*Z*,3*E*-hexadienyl)-3-pyrrolidineacetic acid (domoic acid), *RS*-α-Amino-3-hydroxy-5-methyl-4-isoxazolepropionic acid (RS-AMPA), *N*Methyl-D-aspartic acid (NMDA), 4-(8-Methyl-9*H*-1,3-dioxolo[4,5-*h*][2,3]benzodiazepin-5-yl)-benzenamine dihydrochloride (GYKI-52466 hydrochloride), bicuculline methochloride, MK801, (5*S*,10*R*)-(+)-5-Methyl-10,11-dihydro-5*H*-dibenzo[*a*,*d*]cyclohepten-5,10-imine maleate; S-5-iodowillardine, 1-[6-[[(17β)-3-Methoxyestra-1,3,5(10)-trien-17-yl]amino]hexyl]-1*H*-pyrrole-2,5-dione (U73122), Ro32-0432, 3-[(8*S*)-8-[(Dimethylamino)methyl]-6,7,8,9-tetrahydropyrido[1,2-*a*]indol-10-yl]-4-(1-methyl-1*H*-indol-3-yl)-1*H*-pyrrole-2,5-dione hydrochloride, CNQX and NBQX were purchased from Tocris Bioscience (Ellisville, MO). 9-oxo-11α,15S-dihydroxyprosta-5Z,13E-dien-1-oic acid (PGE2), 9-oxo-11α,15S-dihydroxy-17-phenyl-18,19,20-trinorprosta-5Z,13E-dien-1-oic acid (17 phenyl trinor PGE2, 17-PT), 9α,11α,15S-trihydroxy-prosta-5Z, 13E-dien-1-oic acid ($PGF2_{\alpha}$), 9α,11α,15R-trihydroxy-17-phenyl-18,19,20-trinor-prost-5Z-en-1-oic acid, isopropyl ester (latanoprost), 9-oxo-11α,16S-dihydroxy-17-cyclobutyl-prost-13E-en-1-oic acid, methyl ester (butaprost), 8-chloro-2-[1-oxo-3-(4-pyridinyl)propyl]hydrazide-dibenz[b, f][1, 4]oxazepine-10(11H)-carboxylic acid, monohydrochloride (SC-51089), 8-chloro-dibenz[b,f][1, 4]oxazepine-10(11H)-carboxy-(2-acetyl)hydrazide (SC-19220) and 6-isopropoxy-9-oxoxanthene-2-carboxylic acid (AH-6809) were purchased from Cayman Chemicals (Ann Arbor, MI). Protein kinase inhibitors (lavendustin A, staurosporine, calphostin C) and forskolin were purchased from Calbiochem (La Jolla, CA). Phorbol 12-myristate 13-acetate (PMA) and 1,2-Bis(2-aminophenoxy)ethane-N,N,N′,N′-tetraacetic acid tetrakis(acetoxymethyl ester) (BAPTAAM) were purchased from Sigma (St. Louis, MO). Okadaic acid (OKA) was from LC Laboratories/Alexis (Switzerland). 1-[6-[[(17*β*)-3-Methoxyestra-1,3,5(10)-trien-17-yl]amino]hexyl]-2,5-pyrrolidinedione (U73343) was purchased from BioMol (Plymouth Meeting, PA). D-(-)-2-Amino-5-phosphonopentanoic acid (D-AP5) was purchased from Ascent Scientific (Princeton, NJ). Molecular biology reagents and restriction enzymes were purchased from New England Biolabs (Ipswich, MA) and Promega (Madison, WI). PGE2, $PGF2_{\alpha}$, 17 phenyl trinor PGE2, latanoprost, butaprost, SC-51089, SC-19220, AH-6809, BAPTA-AM, U73122, U73343, lavendustin A, calphostin C, staurosporine, PMA, forskolin (Frosk), CNQX, NBQX and okadaic acid were dissolved in dimethylsulfoxide (DMSO) as stocks and mixed with the recording solution reaching a final concentration as indicated in the results. The final DMSO concentration was ≤ 0.2%, which had no effect on responses. Other chemicals were dissolved in doubly distilled water or experimental solutions.

Data analysis

Data analysis for in vivo kainate experiments and intracellular calcium detection was performed with Microsoft Excel and Origin (Microcal Software, Northampton, MA). Data

analysis for oocyte recording was performed using pClamp and Clampfit 9 (Axon Instruments, Foster City, CA) as well as Origin. Data are presented as means ± standard error. Statistical analysis was performed with Microsoft Excel or GraphPad Prism version 4 (GraphPad software, San Diego, CA). Student's *t* test or one-way ANOVA (with Bonferroni or Dunnett's post tests) of selected means were performed as appropriate. Fisher's exact test was used to compare mortality rates in the two genotypes. The differences were considered to be statistically significant if $p < .05$.

RESULTS

EP1 disruption reduces the probability of entering status epilepticus in kainate-treated mice

The EP1 receptor has been shown to contribute to cellular toxicity and death in rodent models of ischemic stroke and toxin-induced Parkinsonism (Kawano et al., 2006; Ahmad et al., 2006; Ahmad et al., 2013). Hippocampal expression of the EP1 receptor was verified by RTPCR on RNA extracted from eight untreated wildtype C57BL/6 mice (not shown), consistent with a previous report by Zhu et al. (2005). We optimized a mouse kainic acid induced seizure model to investigate the importance of EP1 on seizure threshold, status epilepticus onset and acute seizure induced mortality. Adult male wildtype (WT, C57BL/6CR) mice and age-matched EP1 knockout (EP1-KO) mice of the same background were injected subcutaneously (s.c.) with a single dose of kainic acid (5, 10, 20, 30, or 40 mg/kg) and monitored for a minimum of 6 hours. The doses were separated into low (5, 10 mg/kg), intermediate (20 mg/kg) and high (30, 40 mg/kg). The seizure behavior of the mice was recorded every 5 min for 80-90 min according to a Racine scale modified for kainic acid (in materials and methods). Wildtype and EP1-KO mice developed behavioral seizures with similar sensitivity to kainate (Figure 1A). However, following 20 mg/kg kainate, nearly half of the wildtype mice (47%, n=17) entered status epilepticus as defined by continuous non-remittent seizure activity, whereas none of the EP1-KO mice (n=16) entered into status epilepticus ($p = .003$, Fisher's exact test) (Figure 1B). Likewise, at 30 and 40 mg/kg kainic acid a higher proportion of the wildtype mice entered status epilepticus, with significance being reached at 40 mg/kg ($p = .04$, Fisher's exact test) (Figure 1B). A plot showing the percent of mice that entered into status epilepticus as a function of dose of kainic acid injected revealed a right shift in the dose response curve for EP1-KO mice with a difference in the ED_{50} for kainic acid (21.7 mg/kg for wildtype vs. 32.4 for EP1-KO), suggesting that preventing EP1 receptor activation reduces the probability for mice to enter status epilepticus (Figure 1B).

Similarly, when the data of mice injected with the intermediate and high doses were pooled, a higher proportion of wildtype mice entered status epilepticus (73% for wildtype, n=44 vs. 36% for EP1-KO, n=39; $p = .001$, Fisher's exact test) (Figure 1C) and a higher mean behavioral score was measured in wildtype mice between 60 and 80 minutes following injection of kainic acid (Figure 1D). The latency to enter status epilepticus following subcutaneous kainic acid (40 mg/kg) was also shorter for wildtype mice (mean 25 min) compared to EP1-KO mice (mean 50 min) (Figure 1E). Mice that entered status epilepticus, however, showed no difference in acute mortality between wildtype and EP1-KO mice as

measured within a six hour time period (50% for wildtype, n=32 vs. 43% for EP1-KO, n=14, p =.75 by Fisher's exact test) (Figure 1F), suggesting that the mice experienced a similar seizure intensity. Taken together, these results suggest that the EP1 receptor promotes the transition of kainate-treated mice from seizures to status epilepticus, but does not modify seizure threshold or the survival of mice that do enter status epilepticus.

Mice that experience more than 60 minutes of status epilepticus usually lose body weight for the first two days (Jiang et al., 2013). The weight of wildtype and EP1-KO mice was recorded just prior to a subcutaneous injection of saline or a high concentration of kainic acid and again 24 hours later. Saline injection caused no significant weight change for either wildtype or EP1-KO mice the day after injection (+2.5 ± 1% for wildtype, n=8 vs. +0.4 ± 1.3% for EP1-KO, n=12; p =.3, t test). Likewise, both wildtype and EP1-KO mice that entered status epilepticus after injection of a high concentration of kainic acid (30 or 40 mg/kg) experienced a similar weight loss (−10 ± 2% for wildtype, n=12; −8 ± 1% for EP1-KO, n=10; p =.4, t test), which is consistent with the notion that those wildtype and EP1-KO mice that entered status epilepticus after kainic acid experienced similar status epilepticus intensity. Reinforcing this idea are the observations that wildtype and EP1-KO mice administered kainate intraperitoneally experienced the same duration of status epilepticus and the same weight loss (Figure 1G, H).

EP1 ablation reduces hippocampal neurodegeneration after status epilepticus

In wildtype mice a single subcutaneous injection of kainic acid at a concentration ≥20 mg/kg often induced status epilepticus. The intensity of the seizures following the onset of status epilepticus eventually waned over time and the mice recovered overnight. In contrast to the high delayed mortality observed with pilocarpine (Jiang et al. 2013), mice that survived the acute episode of status epilepticus elicited by kainic acid typically survived the next four days. On the fourth day the mice were sacrificed. RT-PCR analysis on all 14 brains taken from EP1-KO mice that experienced status epilepticus showed a targeted gene insertion used to disrupt the EP1 gene (584 bp amplicon), and also the absence of a 272 bp endogenous PCR product that indicates a wildtype genotype (Figure 2A). By comparison the brains of three wildtype mice produced RT-PCR products indicative of an intact EP1 gene (Figure 2A).

Status epilepticus induced by injection of intermediate to high doses of kainic acid produces a characteristic pattern of neuron loss in the hippocampus of adult rodents (Nadler et al., 1978; Sperk et al., 1983; Wang et al., 2005). FluoroJade B staining was performed on hippocampal sections taken from the brains of mice four days following status epilepticus induced by a single subcutaneous injection of kainic acid at a concentration ≥20 mg/kg to quantify the degree of neuron injury. Coronal sections (8 μm) revealed robust neurodegeneration in the hippocampus of wildtype mice that entered status epilepticus and survived four days (Figure 2B). The number of FluoroJade B positive cells in the CA1 layer was significantly lower in EP1-KO mice compared to wildtype mice (average of 9 FluoroJade positive cells per hippocampal section for wildtype, n=11 vs. 0 FluoroJade positive cells for EP1-KO, n=8) (p =.04, t test) (Figure 2C). A strong trend for reduced neurodegeneration in EP1-KO mice was also observed in the CA3 region (average of 14

FluoroJade positive cells per hippocampal section for wildtype, n=11 vs. 3 FluoroJade positive cells for EP1-KO, n=8), although statistical significance was not attained (p =.11, t test) (Figure 2C). Mice with a genetic deletion of the EP1 receptor had a similar low degree of neurodegeneration in the hilus as wildtype mice (0.3 ± 0.1 cells per section for wildtype, n=11 vs. 0 for EP1-KO, n=8, p =.12, t test) (Figure 2C). Although the degree of neurodegeneration was quite different in the hippocampus of wildtype and EP1-KO mice, the temporal evolution of behavioral seizures was similar in the groups of mice selected for this experiment (Figure 2D), arguing against a cause of lower neurodegeneration being less intense status epilepticus in the EP1-KO. No neurodegeneration was observed in mice that did not enter into status epilepticus (not shown). Taken together, these data indicate that the presence of the EP1 receptor contributes to neurodegeneration in mice following kainic acid induced status epilepticus, even when mice are matched for seizure severity during status epilepticus.

The EP1 receptor contributes to the inflammatory response following status epilepticus

A robust inflammatory reaction occurs in the brains of rodents that experience at least one hour of status epilepticus (Sharma et al., 2009; Serrano et al., 2011; Jiang et al., 2013). This inflammatory reaction is partly mediated by the inducible cyclooxygenase-2 (COX-2) enzyme and subsequent activation of the EP2 receptor for PGE2, as the mRNA level of many pro-inflammatory genes that are normally up regulated following status epilepticus is blunted in mice that lack a functional COX-2 gene in principle forebrain neurons (Serrano et al., 2011), and in mice following systemic administration of an EP2 antagonist beginning 4 hr after SE onset (Jiang et al., 2013). To gain insight into a potential mechanism by which the EP1 receptor could accentuate excitotoxicity and to determine whether EP1 contributes to seizure-induced neuroinflammation, we investigated the expression profile of a panel of inflammatory mediators in wildtype and EP1-KO mice following status epilepticus. qRT-PCR was carried out to measure the level of glial cell markers and 11 inflammatory mediators (bold and underlined in Table 2) that are upregulated in the mouse brain following pilocarpine induced status epilepticus (Serrano et al., 2011; Jiang et al., 2013). Of the 11 inflammatory mediators tested in this experiment CCL2, CCL3, CCL4, IL-1β and IL-6 are all predominantly proinflammatory cytokines. TGFβ1 and CXCL10 have mixed pro-inflammatory and anti-inflammatory actions. COX-2, iNOS, gp91phox and BDNF are modulators of inflammation. For this experiment four groups of mice were investigated: wildtype and EP1-KO mice injected i.p. with saline or 30 or 40 mg/kg kainic acid. To attain a high proportion of mice in status epilepticus, wildtype and EP1-KO mice were administered an initial intraperitoneal dose of 30 mg/kg and 40 mg/kg kainic acid, respectively. Both wildtype and EP1-KO mice were boosted with 10 mg/kg when necessary to attain status epilepticus. The initial i.p. dose of kainic acid was lower in the wildtype compared to the EP1-KO mice, and consequently the temporal evolution of seizure activity in the wildtype was slower (Figure 3D). Only kainate-treated mice that experienced at least 90 minutes of behavioral status epilepticus were used for this experiment. The variation of expression of individual transcripts from mice of the same genotype and treatment was low, with coefficients of variation of ΔCT ranging from 1.3 to 5.2%. The mRNA levels of these inflammatory mediators in wildtype and EP1-KO mice were almost identical in saline injected controls (Figure 3A). The wildtype mice (n≥7) showed increased mRNA levels in

10 out of 11 inflammatory mediators one day after kainate induced status epilepticus, including 49-fold for CCL2, 34-fold for CXCL10, 23-fold for CCL4, and 19-fold for CCL3 (Figure 3B). However, in the EP1-KO mice (n=8) the upregulation of these inflammatory mediators was blunted (Figure 3B, C). The average change of all 11 inflammatory mediators combined was lower in the EP1-KO mice (13 ± 5 fold over control for wildtype vs. 5 ± 2 fold for EP1-KO, p=.027 by paired t test, n=11 mediators). The upregulation of five inflammatory mediators was reduced by greater than 65% in the EP1-KO mice, including CCL2, CCL3, CCL4, IL-6 and COX-2 (Figure 3C). BDNF and TGFβ1 were also significantly blunted in the EP1-KO mice compared to wildtype, being reduced by 46% and 36%, respectively.

Experiments were then performed to determine the features of glial activation as it is known that astrogliosis and microgliosis are prominent in mice following status epilepticus (Borges et al., 2003; Serrano et al., 2011). The mRNA levels of astrocytic GFAP and microglia IBA1 were measured in brain one day after status epilepticus. GFAP mRNA was significantly induced and to the same degree in wildtype and EP1-KO mice that experienced status epilepticus compared to saline controls [4.7 ± 0.6 (n=8) fold induction for wildtype vs 4.7 ± 0.7 (n=8) fold induction for EP1-KO; p =1, t test]. However, in contrast to the delayed induction of IBA1 (a marker of activated microglia) after pilocarpine in wildtype mice (Borges et al., 2003; Serrano et al., 2011), in the EP1-KO mice a small increase was observed in the mRNA levels of IBA1 one day after kainate induced status epilepticus [1.0 ± 0.1 (n=8) fold induction for wildtype vs 1.6 ± 0.2 (n=8) fold induction for EP1-KO; p = .01, t test].

The mRNA levels of astrocytic GFAP were measured in the half brains of a separate group of mice that experienced status epilepticus 4 days earlier. GFAP mRNA remained significantly elevated 4 days later, but was drastically reduced in EP1-KO mice that experienced status epilepticus compared to saline controls [3.5 ± 0.6 (n=6) fold induction for wildtype vs 0.6 ± 0.06 (n=6) fold reduction for EP1-KO; p =.0004, t test]. Fluorescent GFAP immunohistochemistry performed on coronal hippocampal sections taken from the other half of the brains of these mice four days after kainate induced status epilepticus revealed significantly more astrocyte cell body swelling indicative of astrogliosis in the CA3 region of the hippocampus of wildtype mice compared to EP1-KO mice (Figure 3E-G).

The effect of EP1 on cytokine production following KA treatment is not a general effect on inflammation as an EP1 agonist does not potentiate the effect of LPS/IFNγ on cytokine burst in cultured classically-activated microglia (Quan et al., 2013). The seizure-induced upregulation of these inflammatory mediators was reduced in the EP1-KO mice despite the EP1-KO mice reaching status epilepticus faster than wildtype mice in this experiment as revealed by the temporal evolution of seizure activity for all mice used in this experiment (Figure 3D). Together, these data suggest that the EP1 receptor contributes significantly to the inflammatory reaction and gliosis observed the days following kainic acid induced status epilepticus.

Activation of EP1 potentiates kainate receptor activation in cortical cultures

Thus far we have shown that the EP1 receptor contributes to neurotoxicity and selective aspects of neuroinflammation produced by kainic acid. However, the molecular mechanism by which this occurs remains unknown. In a recent study (Rojas et al., 2013) we demonstrated that activation of native kainate receptors in primary neuron-dense cultures leads to a detectable change in intracellular calcium that can be quantified with Ca^{2+} sensing dyes. We demonstrated the presence of kainate receptor subunits and showed that Gαq-coupled metabotropic glutamate receptors could potentiate the activation of heteromeric kainate receptors, but not NMDA or AMPA receptors. In order to determine whether native kainate receptors are also modulated by the EP1 receptor, we first measured intracellular Ca^{2+} following kainate receptor activation in cortical cultures from rats and mice using a fluorescent Ca^{2+} sensing dye (Fluo-4) and a FLEXstation 96-well fluorometer. As the hippocampus was a focus of seizure pathology in the current study efforts were made to measure intracellular calcium levels in hippocampal cultures, however due to a limited ability to obtain sufficient hippocampal neurons from rat pups we carried out most of these experiments using cortical cultures; the high affinity kainate receptor subunits (GluK4, GluK5) are also present in rat cultured cortical neurons (Rojas et al., 2013). Since after 7 days *in vitro* the neuron dense cultures also contained a few GFAP positive astrocytes (Figure 4A), we performed experiments to determine whether kainate receptor Ca^{2+} transients are generated by activation of neuronal or glial kainate receptors. Conversely, glial cultures containing dense GFAP positive astrocytes also contained a sparse number of MAP2 positive neurons after 20 days in vitro (Figure 4B). Neither astrocyte-dense nor neuron-dense cultures contained viable microglia or endothelial cells as judged by immunocytochemistry with the microglia marker Iba1 or the endothelial cell marker CD31 (data not shown).

Kainate receptors in culture were isolated pharmacologically by blocking NMDA, AMPA, and $GABA_A$ receptors with selective inhibitors (10 μM MK801 and 100 μM each of D-AP5, GYKI52466 and bicuculline, respectively). In the presence of these inhibitors bath application of domoic acid (a kainate receptor agonist) increased cytosolic calcium in a concentration dependent manner in neuron dense cultures (Figure 4C). Although cytosolic calcium was also increased in a concentration dependent manner in astrocyte-dense cultures the peak calcium signal in these cultures was significantly lower than that in the neuron-dense cultures (Figure 4C). Together with the observation of sparse astrocytic contamination in the neuron-dense cultures, we conclude that the kainate receptor calcium transient observed in the neuron-dense cultures is of neuronal origin.

In the neuron dense cultures bath application of AMPA (50 μM) in the presence of selective NMDA, AMPA, and $GABA_A$ receptor inhibitors increased cytosolic Ca^{2+} in cortical cultures (Figure 5A). We chose AMPA as an agonist for the calcium assays because in the presence of the cocktail of ionotropic receptor blockers AMPA is a non-desensitizing agonist of heteromeric but not homomeric kainate receptors (Bettler and Mulle, 1995; Lerma et al., 2001; Traynelis et al., 2010). This concentration of AMPA was chosen because it produced large currents from rat heteromeric GluK2/GluK5 expressed in *Xenopus* oocytes and was near the maximally effective concentration (Mott et al., 2010). The AMPA induced

rise in intracellular calcium in rat cortical cultures is attributed to kainate receptors as we previously ruled out the involvement of AMPA receptors or voltage dependent calcium channels (Rojas et al., 2013). Following application of 1 μM PGE2, the increase in cytosolic Ca^{2+} after AMPA exposure was potentiated to 151 ± 5 % compared to vehicle in rat neuron-dense cortical cultures ($p < .01$, oneway ANOVA with Dunnett's post hoc test, n = 22), but not in rat astrocyte-dense cultures (Figure 5B, C). Interestingly, application of 1 μM 17-phenyl-trinor (17-PT, an EP1 and EP3 receptor agonist) also potentiated the kainate receptor dependent increase in intracellular Ca^{2+} in rat neuron-dense cultures to 141 ± 10 % ($p < .05$, one-way ANOVA with Dunnett's post hoc test, n = 15) (Figure 5A, B). The potentiation of kainate receptors by PGE2 and 17-PT was concentration dependent (Figure 5B) and was half-maximal at approximately 100 nM PGE2.

To determine whether the EP1 receptor was necessary for the PGE2 induced potentiation of kainate receptors we cultured cortical neurons from EP1-KO mice. Potentiation following exposure to 100 nM PGE2 was absent in cortical cultures obtained from EP1 lacking (EP1-KO) mice [151 ± 7 % (n=6) for wildtype vs 104 ± 6 % (n=7) for EP1-KO; $p < .0003$, *t* test] (Figure 5C), confirming that EP1 receptor activation mediates the potentiation of native kainate receptors by PGE2. Furthermore, activation of other prostaglandin receptors like EP2 with butaprost (1 μM) and FP using PGF2α (1 μM) or latanoprost (1 μM) failed to reproduce the same potentiation seen with PGE2 (Figure 5C) whereas pretreatment with a cocktail of EP1 receptor antagonists (10 μM AH-6809, 10 μM SC-19220, 10 μM SC51089) strongly attenuated the potentiation of heteromeric kainate receptors in cortical cultures by both 100 nM PGE2 and 100nM 17-PT [104 ± 8% of control, n = 10 for PGE2; 100 ± 10% of control, n = 10 for 17-PT] (Figure 5D). Prior exposure to this cocktail of EP1 receptor antagonists did not affect the baseline calcium signal. In the presence of the NMDA, AMPA and $GABA_A$ inhibitor cocktail, both PGE2 and 17-PT also potentiated the rise in cytosolic calcium induced by kainic acid [122 ± 4% (n=13) for PGE2 and 126 ± 6% (n=13) for 17-PT (Figure 5E).

Protein kinase activators and inhibitors were used to investigate the molecular basis for potentiation of native kainate receptors as activation of EP1 triggers an intracellular signaling cascade that results in the upregulation of phospholipase C, Ca^{2+}, protein kinase C (PKC) and tyrosine kinases (Breyer et al., 1996). Activation of PKC by PMA (100 nM) potentiated the kainate receptor dependent increase in cytosolic Ca^{2+} in rat cortical cultures by 136 ± 6% of control, n = 14 (Figure 5E). Conversely, pretreatment of rat neuron dense cortical cultures with the protein kinase C inhibitor Ro32-0432 (4 μM) blocked the PGE2 induced potentiation of kainate receptors (108 ± 7 % of control, n = 6) (Figure 5F), suggesting that protein kinase C is likely to be involved in this modulation. Unfortunately, pretreatment with lavendustin A (a Src tyrosine kinase inhibitor) or genistein (a general tyrosine kinase inhibitor) altered the baseline Ca^{2+} in the cortical cultures, precluding use of these compounds. Taken together, these data suggest that native kainate receptors in cortical cultures are potentiated by activation of EP1 receptors in a PKC dependent manner.

Activation of EP1 but not EP2 potentiates recombinant heteromeric kainate receptors

We explored the kainate receptor subunit composition sensitive to prostaglandin receptor signaling by co-expressing specific kainate receptors along with either the EP1 or EP2 receptor in *Xenopus* oocytes. In oocytes co-expressing kainate receptors with EP1, typical inward currents were elicited by 30 μM AMPA for heteromeric kainate receptors (assemblies of GluK2 and either GluK4 or GluK5 subunits), and by 30 μM domoic acid for homomeric GluK1 and GluK2 kainate receptors (Figure 6A). Agonist responses were absent in uninjected oocytes or oocytes injected with vehicle only (no mRNA). After baseline responses to repeated agonist exposure stabilized, PGE2 was applied for 2 minutes. Following EP1 activation GluK2/GluK5 receptors showed significant potentiation (135 ± 6% of baseline current, n = 13; $p < .001$ by oneway ANOVA with posthoc Bonferroni) (Figure 6A, B). The GluK2/GluK4 receptors also showed potentiation following EP1 receptor activation, however, to a lesser degree than GluK2/GluK5 and failed to reach statistical significance 116 ± 5% (n = 5) (Figure 6A, B). By contrast, both the DMSO vehicle and EP1 activation revealed a rundown in the GluK2 current (Figure 6A, B). Thus, potentiation was only observed upon activation of the EP1 receptor expressed with heteromeric kainate receptors. No potentiation was observed in oocytes co-expressing GluK2/GluK5 and EP1 following exposure to the DMSO vehicle used to prepare both PGE2 and 17-PT (Figure 6B).

The EP1 receptor is a GPCR coupled to $G\alpha_q$ (Breyer et al., 1996). To determine whether prostanglandin receptors coupled to a different G-protein also modulate kainate receptors, similar experiments were performed on oocytes co-expressing heteromeric kainate receptors with EP2 (a prostaglandin receptor that is activated by PGE2 but couples with $G\alpha_s$). In oocytes co-expressing GluK2/GluK5 and EP2, perfusion with PGE2 did not augment kainate receptor mediated currents [107 ± 3 % of control (n = 10)] (Figure 6B) suggesting that the $G\beta\gamma$ subunit of the G-protein does not influence GluK2/GluK5. The largest potentiation of kainate receptor currents was observed following bath application of PGE2 in oocytes co-expressing GluK2/GuK5 along with EP1 (Figure 6B). The EP1-mediated potentiation of heteromeric GluK2/GluK5 currents occurred within the first two minutes after exposure to PGE2 and persisted for at least 12 minutes (Figure 6C). We have recorded potentiation lasting up to 25 minutes however recording stability complicated the data from longer recordings. Therefore, all experiments involving EP1 activation were carried out with a minimum exposure of 2 minutes and a maximum of 15 minutes. The potentiation of the GluK2/GluK5 receptor by EP1 receptor activation was concentration dependent (Figure 6D).

To determine whether EP1 activation alters the potency with which AMPA activates heteromeric kainate receptors, AMPA concentration-response relationships with or without preceding activation of EP1 were compared. Activation of EP1 by PGE2 increased the kainate receptor current across a range of AMPA concentrations, but did not alter AMPA potency (Figure 7A). EP1 receptor activation by PGE2 also potentiated currents activated by another non-desensitizing kainate receptor agonist, S-5-iodowillardine (127 ± 7 % of control; n = 12) (Figure 7B, C). The specificity for activation of EP1 leading to kainate receptor potentiation was confirmed by pre-treatment of oocytes with an EP1 selective

(SC-51089) and non-selective (AH-6809) antagonist. Prior exposure of oocytes expressing GluK2/GluK5+EP1 to SC-51089 or AH-6809 strongly attenuated the potentiation by PGE2 [108 ± 4 % of control (n = 7) for SC51089; 87 ± 2 % of control (n = 11) for AH-6809] (Figure 7B).

Activation of EP1 by the specific receptor agonist 17-phenyl-trinor also potentiated GluK2/GluK5 currents in a similar manner as PGE2 [131 ± 9% of control (n = 5)] (Figure 7D). Interestingly, 17-PT also potentiated GluK2/GluK4 currents to a similar degree as PGE2 (Figure 7D). 17-PT failed to potentiate GluK2/GluK4 and GluK2/GluK5 in the absence of EP1 (Figure 7D). We conclude that heteromeric kainate receptors containing GluK2 in combination with GluK4 or GluK5 subunits are modulated by the EP1 receptor, with heteromers containing GluK5 showing the highest potentiation.

Requirement for PLC activation and Ca^{2+} mobilization

Ligand binding to the EP1 receptor sets in motion an intracellular second messenger cascade that involves activation of molecules such as $G\alpha_q$, phospholipase C, Ca^{2+} and protein kinase C. All of these mediators were necessary for the potentiation of GluK2/GluK5 receptors by EP1. The phospholipase C (PLC) inhibitor U73122 (10 μM) abolished EP1 mediated GluK2/GluK5 potentiation by exposure to 2 μM PGE2 compared to oocytes exposed to its inactive isomer U73343 (10 μM) [93 ± 2% of control, n = 6 for U73122; 148 ± 6% of control, n = 5 for U73343; **** $p < .001$, *t*-test]. The Ca^{2+} assay experiments with rat cortical cultures suggested that a downstream consequence of activation of EP1 is a rise in intracellular Ca^{2+}. During the recordings in oocytes large calcium activated Cl^- currents were observed following activation of the EP1 receptor that were absent following activation of EP2. To determine whether an increase in intracellular Ca^{2+} is required for the EP1 mediated potentiation of GluK2/GluK5, oocytes co-expressing GluK2/GluK5 and EP1 were pre-incubated with the cell membrane permeable Ca^{2+} chelator BAPTA-AM (100 μM) prior to recording. BAPTA-AM eliminated the potentiation of kainic acid responses by EP1 [133 ± 6%, n = 8 for control; 100 ± 5%, n = 7 for BAPTA-AM; *** $p < .005$, *t* test] (Figure 8A). Together, these results suggest that following activation of EP1 a signaling pathway involving both PLC and an increase in intracellular Ca^{2+} are necessary for potentiation of the GluK2/GluK5 receptor.

PLC activation and an increase in intracellular Ca^{2+} are together required for the activation of protein kinase C (PKC). In Figure 5F we showed that a PKC inhibitor could prevent potentiation by EP1 of heteromeric kainate receptors in cortical neurons. To confirm whether PKC is involved in the potentiation of GluK2/GluK5 receptors by EP1 activation, the effects of the general protein kinase inhibitor staurosporine and the selective PKC inhibitor calphostin-C were explored. Pre-incubation of oocytes with staurosporine (300 nM) caused a near complete attenuation of the EP1 mediated effect to 107 ± 4% of control (n = 6) (Figure 8B) ($p<.05$, oneway ANOVA with Dunnett's post hoc comparison). Pre-treatment with calphostin-C (3 μM) also attenuated the PGE2-mediated kainic acid potentiation to 114 ± 5% of control (n = 6) (Figure 8B). We conclude that PKC activation is a necessary step for the potentiation.

Src tyrosine kinases have been shown to mediate the potentiation of NMDA receptors following $G\alpha_q$ coupled GPCR activation (Wang and Salter, 1994; Chen and Leonard, 1996; Kohr and Seeburg, 1996). However, exposure of oocytes to lavendustin A, a potent and specific inhibitor of Src tyrosine kinase, had no effect on the potentiation of heteromeric GluK2/GluK5 by EP1 receptor activation (Figure 8B). We previously showed that this concentration of lavendustin A prevents potentiation of NMDA receptors by mGlu1/5 activation (Rojas et al., 2013). Unlike its basal effects on neuron calcium level, lavendustin A had no effect on the basal GluK2/GluK5 currents in the oocytes.

If activation of EP1 results in phosphorylation of GluK2/GluK5, then inhibition of phosphatases may further enhance the effect of PGE2, as shown for the potentiating effect of group I mGlu agonists (Rojas et al., 2013). However, after incubation of oocytes in 100 nM okadaic acid, a cell permeable inhibitor of PP1 and PP2A phosphatases, the average PGE2 induced potentiation of GluK2/GluK5 was not larger (141 ± 10% of control, n=6) (Figure 8C). Indirect activation of protein kinase A (PKA) by forskolin (an adenylate cyclase activator) did not potentiate GluK2/GluK5 suggesting that PKA is not involved in the potentiation seen following EP1 activation (Figure 8C). Taken as a whole, these data suggest that regulation of the heteromeric GluK2/GluK5 by the EP1 receptor is mediated by PKC, but not by PKA or Src tyrosine kinase.

The C-terminus of GluK5 is critical for the potentiation of GluK2/GluK5 receptors

Since potentiation of heteromeric kainate receptors by EP1 is stronger for receptors with GluK5 than those with GluK4 (Figure 6B) and no potentiation was seen in homomeric GluK2 receptors, we examined the role of the intracellular domains of GluK5 in the potentiation. We narrowed our focus to three serine residues (i.e., S833, S836 and S840) in the C-terminus of GluK5 as we recently identified these serines to be collectively critical for the potentiation of GluK2/GluK5 by PKC activation and group I mGlu receptor activation (Rojas et al., 2013). Therefore, we performed similar experiments to determine whether these same three serines are also necessary for the potentiation of GluK2/GluK5 by EP1 receptor activation. We converted all three residues to aspartate to produce constitutively negatively charged residues that might mimic phosphorylation of the receptor. The GluK5 triple aspartate mutant (GluK5-S833D/S836D/S840D; GluK5-TD) was co-injected with GluK2 and EP1 in *Xenopus* oocytes. Subsequently, we tested the effect of EP1 activation by PGE2 on this mutant. The triple aspartate GluK5 mutant (GluK5-TD) failed to be potentiated by exposure to PGE2 when co-expressed with GluK2 and EP1 [101 ± 5% of control, n=11] (Figure 8C). However, mutation of the same three serines in GluK5 to glutamate (GluK5-S833E/S836E/S840E; GluK5-TE) was permissive for PGE2 sensitivity (137 ± 5% of control, n=12) (Figure 8C, D), as it was for mGlu1 activation (Rojas et al., 2013), suggesting that mimicking phosphorylation does not solely depend on the negative charge of the three critical serines. To determine whether other critical GluK5 C-terminal amino acids downstream of these serines contributes to the PGE2 sensitivity of the heteromeric kainate receptor, we coexpressed GluK2 and EP1 with a mutant GluK5 receptor in which the three critical serines were mutated to glutamate and a truncation was introduced after amino acid 884 (GluK5-S833E/S836E/S840E-Δ884; GluK5-TE-D884). We previously showed that combining the truncation after amino acid 884 with the mutation of the three

serines to glutamate reversed the potentiation of the GluK2/GluK5-TE+mGlu1 by ACPD and PMA (Rojas et al., 2013). Here, the mutant receptor GluK2/GluK5-S833E/S836E/S840E-Δ884 displayed inhibition rather than potentiation by PGE2 when coexpressed with EP1 (76 ± 4% of control, n = 13; Figure 8C) suggesting that the three proximal C-terminal serine residues (S833, S836, S840) in GluK5 are necessary for the EP1-mediated potentiation of heteromeric kainate receptors, but other downstream C-terminal residues in GluK5 contribute to the potentiation.

DISCUSSION

Here we show expression of the EP1 receptor in the hippocampus of mice and the functional influence of the EP1 receptor on kainic acid induced seizures. Mice lacking a functional EP1 receptor gene displayed a lower tendency to enter status epilepticus when injected with high concentrations of kainic acid although they exhibited a similar behavioral seizure threshold compared to their wildtype counterparts, suggesting that EP1 receptor activation increases the probability for entry of mice into status epilepticus. Moreover, for EP1-KO and wildtype mice selected for the same behavioral seizure intensity during status epilepticus, the EP1-KO showed a smaller cytokine burst one day later and less neurodegeneration 4 days later. These results together suggest that EP1 activation regulates the response to kainate both directly by increasing the probability to enter status epilepticus, and indirectly by intensifying the consequences of status epilepticus.

Analysis of acute mortality caused by status epilepticus revealed no difference for mice lacking a functional EP1 gene compared to wildtype mice indicating that the EP1 receptor does not contribute to the overall survival of mice. However, we found neuroprotection of hippocampal pyramidal neurons in the CA1 and CA3 layers after status epilepticus in the EP1-KO mouse, which is striking because mice lacking EP1 displayed a similar behavioral seizure phenotype as wildtype mice (Figure 2D). Therefore, EP1 activation during or after status epilepticus appears to contribute to subsequent CA1 and CA3 pyramidal cell neurodegeneration. One day after kainic acid induced status epilepticus in the EP1-KO mouse, we also observed that the induction of 11 inflammatory mediators in the forebrain was blunted. The induction of the pro-inflammatory mediators CCL2, CCL3, CCL4 and IL-6 were strongly attenuated in the EP1-KO mice, suggesting that the robust overall brain inflammation may be reduced in the EP1-KO mice following status epilepticus. COX-2 induction was also significantly reduced in EP1-KO mice suggesting that these early effects might be dependent consequences of COX-2 regulation. Although COX-2 is upstream of the EP1 receptor in the prostaglandin signaling pathway the reduction of COX-2 seen in the EP1-KO mice compared to wildtype following kainate induced status epilepticus is not surprising as it is known that COX-2 is an activity-dependent enzyme, responding to cytoplasmic Ca^{2+} levels that can rise upon activation of the EP1 receptor, or coactivation of EP1 and kainate receptors. In the EP1-KO intracellular Ca^{2+} might not rise high enough during status epilepticus to induce COX-2 to the same extent as in WT mice. In summary, the EP1 receptor partially mediates the robust inflammatory response following kainic acid induced status epilepticus.

The GPCR – $G\alpha_q$ – PKC pathway, activated by mGlu1/5 (Rojas et al., 2013), mAChR (Benveniste et al., 2010) and now EP1, represents a general post-translational regulatory mechanism for heteromeric kainate receptors bearing the GluK4 or GluK5 subunits. The observed EP1-induced and PKC-mediated potentiation of heteromeric GluK2/GluK5 but not homomeric GluK2 strengthens the idea that the GluK5 subunit may be a regulatory subunit in the kainate receptor complex as was shown for heteromeric kainate receptor potentiation by muscarinic M1, M3 and group I mGlu receptors (Benveniste et al., 2010; Rojas et al., 2013). EP1 receptor activation engages this pathway to potentiate heteromeric but not homomeric kainate receptors, pointing to a mechanism by which the potentiation of kainate receptors by EP1 receptor activation likely occurs through phosphorylation by PKC of specific residues in high affinity kainate receptor subunits. Here, we demonstrated that PGE2 potentiates kainate receptor-induced Ca^{2+} signals in neuron rich mouse and rat cortical cultures in a PKC-dependent manner, confirming that EP1 receptor activation potentiates native kainate receptor-mediated calcium signaling.

Key molecules in the EP1 second messenger signaling cascade that are necessary for potentiation of GluK2/GluK5 were identified. We also identified three GluK5 serines located in a membrane-proximal C-terminal domain that, when mutated to the phosphomimetic aspartate and expressed with GluK2, rendered the receptor insensitive to EP1 modulation, as if this construct had been “pre-potentiated”. The peak potentiation of heteromeric kainate receptors following activation of mGlu1 was reached within 3 minutes and then gradually declined (Rojas et al., 2013). This gradual decline of mGlu1 potentiated kainate receptor currents was attributed to the activation of phosphatases as it was absent in cells pre-treated with the phosphatase inhibitor okadaic acid (Rojas et al., 2013). Contrary to potentiation by mGlu1, heteromeric kainate receptor currents potentiated by EP1 continually increased with time (Figure 6C), and pretreatment with okadaic acid did not significantly affect the average peak kainate receptor currents following EP1 activation (Figure 8C). Therefore, unlike the modulation of heteromeric kainate receptors by group I metabotropic glutamate receptors (Rojas et al., 2013), termination of potentiation by EP1 is likely mediated by different phosphatases, which suggests that EP1 activation engages mechanisms in addition to PKC that modulate kainate receptors.

The modulation of NMDA receptors following engagement of a $G\alpha_q$ signaling cascade proceeds through a more elaborate signaling cascade. Activation of mGlu5 or the M1 acetylcholine receptor results in the activation of PKC that subsequently phosphorylates the Src complex protein PYK2, in turn activating Src tyrosine kinase, which phosphorylates a tyrosine residue in the C-terminus of NMDA receptor subunit GluN2B that alters the surface expression of this subunit (MacDonald et al., 2007). Unlike NMDA receptors, the potentiation of heteromeric kainate receptors by EP1 activation appears to be Src independent as it was not affected by pretreatment with lavendustin A (a Src tyrosine kinase inhibitor). This is a key difference in the regulation of kainate and NMDA receptors by $G\alpha_q$ coupled GPCR activation, as ionotropic glutamate receptors are interwoven in multiple membrane protein complexes that alter receptor function (Rojas and Dingledine, 2013).

Heteromeric and homomeric kainate receptors appear to have distinct post-translational modification potential. For example, homomeric GluK2 receptors are phosphorylated by

both PKC and PKA (Nasu-Nishimura et al., 2010; Konopacki et al., 2011; Chamberlain et al., 2012; Raymond et al., 1993; Wang et al., 1993; Raymond et al., 1994; Traynelis and Wahl, 1997; Kronreich et al., 2007), whereas heteromeric GluK2 containing kainate receptors are modulated by activation of PKC but not PKA (Figure 8B, C and Rojas et al., 2013). In addition to regulation by PKA and PKC, homomeric GluK2 receptors can also be SUMOylated at a C-terminal consensus site resulting in receptor endocytosis and consequent altered synaptic excitability and transmission (Martin et al., 2007; Wilkinson et al., 2008; Konopacki et al., 2011; Chamberlain et al., 2012; Wilkinson et al., 2012), as well as palmitoylated at C-terminal cysteine residues (Pickering et al., 1995). These post-translational modifications of GluK2 are not mutually exclusive. In fact, phosphorylation of the C-terminus of GluK2 by PKC promotes both palmitoylation and SUMOylation, suggesting a functional network of PKC, SUMOylation and palmitoylation that regulates surface expression of GluK2 containing kainate receptors (Pickering et al., 1995; Konopacki et al., 2011). Although homomeric GluK2 receptors are SUMOylated and palmitoylated, little is known regarding these post-translational modifications of heteromeric GluK2 containing receptors (e.g. GluK2/Gluk5 and GluK2/GluK4). Further investigation is necessary to determine whether heteromeric GluK2 containing receptors are regulated by SUMOylation and palmitoylation and whether there is a subsequent change in receptor trafficking or function.

In summary, EP1 signaling modulates heteromeric kainate receptors at multiple steps, both sensitizing mice to kainate-evoked status epilepticus and, separately, exacerbating the downstream consequences of status epilepticus. These results, together with those of Serrano et al. (2011) and Jiang et al. (2013), suggest that activation of both EP1 and EP2 receptors by COX-2 derived PGE2 contributes to neuropathology after status epilepticus in mice. Heteromeric kainate receptors consisting of GluK2 and a high affinity kainate receptor subunit (GluK4 or GluK5) are potentiated by activation of EP1 receptors in a PKC dependent manner, likely via phosphorylation of critical residues located in the membrane-proximal C-terminus of GluK4 or GluK5. The regulation described here confers distinct functional properties to heteromeric kainate receptors that may serve as a convergent molecular basis for kainate receptor and prostanoid receptor cross-talk. Such cross-talk between ionotropic glutamate receptors and the prostanoid receptors may create novel therapeutic opportunities. Although the roles of prostanoid receptors in temporal lobe epilepsy have not been fully addressed, selective EP1 receptor inhibitors could prove useful as a therapeutic strategy for status epilepticus and associated neuropathologies, as well as for other disorders dependent on kainate receptor activation, such as neuropathic pain. Alternatively, given the similarities in effects of EP1 ablation and EP2 antagonism, it could be worthwhile to develop inhibitors of the *PTGES* prostaglandin synthase.

Acknowledgments

This work is supported by NIH RO1 NS036604, U01 NS058158 (RD), P20 NS080185 and T32 DA15040 (AR), and in part by the neuronal imaging core facilities grant P30 NS055077.

Abbreviations

GluK	kainate receptor
PGE2	prostaglandin E2
$PGF2_{\alpha}$	Prostaglandin F2α
EP1	prostaglandin E2 receptor 1
EP2	prostaglandin E2 receptor 2
EP1-KO	prostaglandin E2 receptor 1 knockout mice
WT	C57Bl/6 wildtype mice
EC_{50}	half maximal effective concentration
ED_{50}	effective dose for 50% of subjects
PKC	protein kinase C
PKA	protein kinase A
HBSS	Hank's balanced salt solution
ANOVA	analysis of variance
KAR	kainate receptor
KA	kainic acid
Dom	domoic acid
SE	status epilepticus
GFAP	Glial fibrillary acidic protein
MAP2	microtubule-associated protein 2
Iba1	ionized calcium-binding adapter molecule 1
CA1	*Cornu Ammonis* 1
CA3	*Cornu Ammonis* 3
CT	cycle threshold
Con	control

REFERENCES

Ahmad AS, Saleem S, Ahmad M, Dore S. Prostaglandin EP1 receptor contributes to excitotoxicity and focal ischemic brain damage. Toxicol Sci. 2006; 89:265–270. [PubMed: 16237196]

Ahmad AS, Maruyama T, Narumiya S, Dore S. PGE2 EP1 receptor deletion attenuates 6-OHDA-induced Parkinsonism in mice: old switch, new target. Neurotox Res. 2013; 23:260–266. [PubMed: 23385625]

Ben-Ari Y, Lagowska J, Tremblay E, Le Gal La Salle G. A new model of focal status epilepticus: intra-amygdaloid application of kainic acid elicits repetitive secondarily generalized convulsive seizures. Brain research. 1979; 163:176–179. [PubMed: 427540]

Benveniste M, Wilhelm J, Dingledine RJ, Mott DD. Subunit-dependent modulation of kainate receptors by muscarinic acetylcholine receptors. Brain research. 2010; 1352:61–69. [PubMed: 20655886]

Bettler B, Mulle C. Review: neurotransmitter receptors. II. AMPA and kainate receptors. Neuropharmacology. 1995; 34:123–139. [PubMed: 7542368]

Borges K, Gearing M, McDermott DL, Smith AB, Almonte AG, Wainer BH, Dingledine R. Neuronal and glial pathological changes during epileptogenesis in the mouse pilocarpine model. Experimental neurology. 2003; 182:21–34. [PubMed: 12821374]

Breyer MD, Jacobson HR, Breyer RM. Functional and molecular aspects of renal prostaglandin receptors. J Am Soc Nephrol. 1996; 7:8–17. [PubMed: 8808104]

Chamberlain SE, Gonzalez-Gonzalez IM, Wilkinson KA, Konopacki FA, Kantamneni S, Henley JM, Mellor JR. SUMOylation and phosphorylation of GluK2 regulate kainate receptor trafficking and synaptic plasticity. Nature neuroscience. 2012; 15:845–852.

Chen C, Leonard JP. Protein tyrosine kinase-mediated potentiation of currents from cloned NMDA receptors. J Neurochem. 1996; 67:194–200. [PubMed: 8666992]

Chen C, Bazan NG. Endogenous PGE2 regulates membrane excitability and synaptic transmission in hippocampal CA1 pyramidal neurons. J Neurophysiol. 2005; 93:929–941. [PubMed: 15653788]

Curras MC, Dingledine R. Selectivity of amino acid transmitters acting at N-methyl-D-aspartate and amino-3-hydroxy-5-methyl-4-isoxazolepropionate receptors. Mol Pharmacol. 1992; 41:520–526. [PubMed: 1372086]

Darstein M, Petralia RS, Swanson GT, Wenthold RJ, Heinemann SF. Distribution of kainate receptor subunits at hippocampal mossy fiber synapses. J Neurosci. 2003; 23:8013–8019. [PubMed: 12954862]

Fukumoto K, Takagi N, Yamamoto R, Moriyama Y, Takeo S, Tanonaka K. Prostanoid EP1 receptor antagonist reduces blood-brain barrier leakage after cerebral ischemia. European journal of pharmacology. 2010; 640:82–86. [PubMed: 20470769]

Guan Y, Zhang Y, Wu J, Qi Z, Yang G, Dou D, Gao Y, Chen L, Zhang X, Davis LS, Wei M, Fan X, Carmosino M, Hao C, Imig JD, Breyer RM, Breyer MD. Antihypertensive effects of selective prostaglandin E2 receptor subtype 1 targeting. The Journal of clinical investigation. 2007; 117:2496–2505. [PubMed: 17710229]

Hellier JL, Patrylo PR, Buckmaster PS, Dudek FE. Recurrent spontaneous motor seizures after repeated low-dose systemic treatment with kainate: assessment of a rat model of temporal lobe epilepsy. Epilepsy Res. 1998; 31:73–84. [PubMed: 9696302]

Huettner JE. Kainate receptors and synaptic transmission. Prog Neurobiol. 2003; 70:387–407. [PubMed: 14511698]

Jiang J, Quan Y, Ganesh T, Pouliot WA, Dudek FE, Dingledine R. Inhibition of the prostaglandin receptor EP2 following status epilepticus reduces delayed mortality and brain inflammation. Proceedings of the National Academy of Sciences of the United States of America. 2013; 110:3591–3596. [PubMed: 23401547]

Jiang J, Ganesh T, Du Y, Thepchatri P, Rojas A, Lewis I, Kurtkaya S, Li L, Qui M, Serrano G, Shaw R, Sun A, Dingledine R. Neuroprotection by selective allosteric potentiators of the EP2 prostaglandin receptor. Proceedings of the National Academy of Sciences of the United States of America. 2010; 107:2307–2312. [PubMed: 20080612]

Kamiya H. Kainate receptor-dependent presynaptic modulation and plasticity. Neurosci Res. 2002; 42:1–6. [PubMed: 11814603]

Kawano T, Anrather J, Zhou P, Park L, Wang G, Frys KA, Kunz A, Cho S, Orio M, Iadecola C. Prostaglandin E2 EP1 receptors: downstream effectors of COX-2 neurotoxicity. Nat Med. 2006; 12:225–229. [PubMed: 16432513]

Kohr G, Seeburg PH. Subtype-specific regulation of recombinant NMDA receptor-channels by protein tyrosine kinases of the src family. The Journal of physiology. 1996; 492(Pt 2):445–452. [PubMed: 9019541]

Konopacki FA, Jaafari N, Rocca DL, Wilkinson KA, Chamberlain S, Rubin P, Kantamneni S, Mellor JR, Henley JM. Agonist-induced PKC phosphorylation regulates GluK2 SUMOylation and kainate

receptor endocytosis. Proceedings of the National Academy of Sciences of the United States of America. 2011; 108:19772–19777. [PubMed: 22089239]

Kornreich BG, Niu L, Roberson MS, Oswald RE. Identification of C-terminal domain residues involved in protein kinase A-mediated potentiation of kainate receptor subtype 6. Neuroscience. 2007; 146:1158–1168. [PubMed: 17379418]

Lerma J. Roles and rules of kainate receptors in synaptic transmission. Nat Rev Neurosci. 2003; 4:481–495. [PubMed: 12778120]

Lerma J, Paternain AV, Rodriguez-Moreno A, Lopez-Garcia JC. Molecular physiology of kainate receptors. Physiol Rev. 2001; 81:971–998. [PubMed: 11427689]

MacDonald JF, Jackson MF, Beazely MA. G protein-coupled receptors control NMDARs and metaplasticity in the hippocampus. Biochimica et biophysica acta. 2007; 1768:941–951. [PubMed: 17261268]

Martin S, Nishimune A, Mellor JR, Henley JM. SUMOylation regulates kainate-receptor-mediated synaptic transmission. Nature. 2007; 447:321–325. [PubMed: 17486098]

Matsuoka Y, Furuyashiki T, Yamada K, Nagai T, Bito H, Tanaka Y, Kitaoka S, Ushikubi F, Nabeshima T, Narumiya S. Prostaglandin E receptor EP1 controls impulsive behavior under stress. Proceedings of the National Academy of Sciences of the United States of America. 2005; 102:16066–16071. [PubMed: 16247016]

Mott DD, Rojas A, Fisher JL, Dingledine RJ, Benveniste M. Subunit-specific desensitization of heteromeric kainate receptors. The Journal of physiology. 2010; 588:683–700. [PubMed: 20026616]

Nadler JV, Perry BW, Cotman CW. Intraventricular kainic acid preferentially destroys hippocampal pyramidal cells. Nature. 1978; 271:676–677. [PubMed: 625338]

Nasu-Nishimura Y, Jaffe H, Isaac JT, Roche KW. Differential regulation of kainate receptor trafficking by phosphorylation of distinct sites on GluR6. The Journal of biological chemistry. 2010; 285:2847–2856. [PubMed: 19920140]

Pickering DS, Taverna FA, Salter MW, Hampson DR. Palmitoylation of the GluR6 kainate receptor. Proceedings of the National Academy of Sciences of the United States of America. 1995; 92:12090–12094. [PubMed: 8618850]

Pinheiro P, Mulle C. Kainate receptors. Cell Tissue Res. 2006; 326:457–482. [PubMed: 16847640]

Quan Y, Jiang J, Dingledine R. EP2 receptor signaling pathways regulate classical activation of microglia. The Journal of biological chemistry. 2013; 288:9293–9302. [PubMed: 23404506]

Racine RJ. Modification of seizure activity by electrical stimulation. II. Motor seizure. Electroencephalogr Clin Neurophysiol. 1972; 32:281–294. [PubMed: 4110397]

Raymond LA, Blackstone CD, Huganir RL. Phosphorylation and modulation of recombinant GluR6 glutamate receptors by cAMP-dependent protein kinase. Nature. 1993; 361:637–641. [PubMed: 8094892]

Raymond LA, Tingley WG, Blackstone CD, Roche KW, Huganir RL. Glutamate receptor modulation by protein phosphorylation. Journal of physiology. Paris. 1994; 88:181–192. [PubMed: 7530547]

Rojas A, Dingledine R. Ionotropic glutamate receptors: regulation by G-protein-coupled receptors. Molecular pharmacology. 2013; 83:746–752. [PubMed: 23348498]

Rojas A, Wetherington J, Shaw R, Serrano G, Swanger S, Dingledine R. Activation of group I metabotropic glutamate receptors potentiates heteromeric kainate receptors. Molecular pharmacology. 2013; 83:106–121. [PubMed: 23066089]

Schmued LC, Albertson C, Slikker W Jr. Fluoro-Jade: a novel fluorochrome for the sensitive and reliable histochemical localization of neuronal degeneration. Brain research. 1997; 751:37–46. [PubMed: 9098566]

Serrano GE, Lelutiu N, Rojas A, Cochi S, Shaw R, Makinson CD, Wang D, FitzGerald GA, Dingledine R. Ablation of cyclooxygenase-2 in forebrain neurons is neuroprotective and dampens brain inflammation after status epilepticus. J Neurosci. 2011; 31:14850–14860. [PubMed: 22016518]

Sharma AK, Searfoss GH, Reams RY, Jordan WH, Snyder PW, Chiang AY, Jolly RA, Ryan TP. Kainic acid-induced F-344 rat model of mesial temporal lobe epilepsy: gene expression and canonical pathways. Toxicol Pathol. 2009; 37:776–789. [PubMed: 19700661]

Shimamura M, Zhou P, Casolla B, Qian L, Capone C, Kurinami H, Iadecola C, Anrather J. Prostaglandin E2 type 1 receptors contribute to neuronal apoptosis after transient forebrain ischemia. Journal of cerebral blood flow and metabolism. 2013; 33:1207–1214. [PubMed: 23632967]

Sperk G, Lassmann H, Baran H, Kish SJ, Seitelberger F, Hornykiewicz O. Kainic acid induced seizures: neurochemical and histopathological changes. Neuroscience. 1983; 10:1301–1315. [PubMed: 6141539]

Stock JL, Shinjo K, Burkhardt J, Roach M, Taniguchi K, Ishikawa T, Kim HS, Flannery PJ, Coffman TM, McNeish JD, Audoly LP. The prostaglandin E2 EP1 receptor mediates pain perception and regulates blood pressure. The Journal of clinical investigation. 2001; 107:325–331. [PubMed: 11160156]

Traynelis SF, Wahl P. Control of rat GluR6 glutamate receptor open probability by protein kinase A and calcineurin. The Journal of physiology. 1997; 503(Pt 3):513–531. [PubMed: 9379408]

Traynelis SF, Wollmuth LP, McBain CJ, Menniti FS, Vance KM, Ogden KK, Hansen KB, Yuan H, Myers SJ, Dingledine R. Glutamate receptor ion channels: structure, regulation, and function. Pharmacol Rev. 2010; 62:405–496. [PubMed: 20716669]

Wang YT, Salter MW. Regulation of NMDA receptors by tyrosine kinases and phosphatases. Nature. 1994; 369:233–235. [PubMed: 7514272]

Wang LY, Taverna FA, Huang XP, MacDonald JF, Hampson DR. Phosphorylation and modulation of a kainate receptor (GluR6) by cAMP-dependent protein kinase. Science. 1993; 259:1173–1175. [PubMed: 8382377]

Wang Q, Yu S, Simonyi A, Sun GY, Sun AY. Kainic acid-mediated excitotoxicity as a model for neurodegeneration. Molecular neurobiology. 2005; 31:3–16. [PubMed: 15953808]

Wilkinson KA, Nishimune A, Henley JM. Analysis of SUMO-1 modification of neuronal proteins containing consensus SUMOylation motifs. Neuroscience letters. 2008; 436:239–244. [PubMed: 18400391]

Wilkinson KA, Konopacki F, Henley JM. Modification and movement: Phosphorylation and SUMOylation regulate endocytosis of GluK2-containing kainate receptors. Communicative & integrative biology. 2012; 5:223–226. [PubMed: 22808340]

Zhen G, Kim YT, Li RC, Yocum J, Kapoor N, Langer J, Dobrowolski P, Maruyama T, Narumiya S, Dore S. PGE2 EP1 receptor exacerbated neurotoxicity in a mouse model of cerebral ischemia and Alzheimer's disease. Neurobiology of aging. 2012; 33:2215–2219. [PubMed: 22015313]

Zhu P, Genc A, Zhang X, Zhang J, Bazan NG, Chen C. Heterogeneous expression and regulation of hippocampal prostaglandin E2 receptors. Journal of neuroscience research. 2005; 81:817–826. [PubMed: 16041798]

Highlights

- Mice lacking EP1 displayed a reduced likelihood to enter status epilepticus.
- EP1 receptor lacking mice had decreased hippocampal neurodegeneration.
- EP1 receptor lacking mice showed a blunted inflammatory response.
- Native and recombinant kainate receptors are potentiated by EP1 activation.
- PKC acting on residues in GluK5 underlie kainate receptor potentiation by EP1.

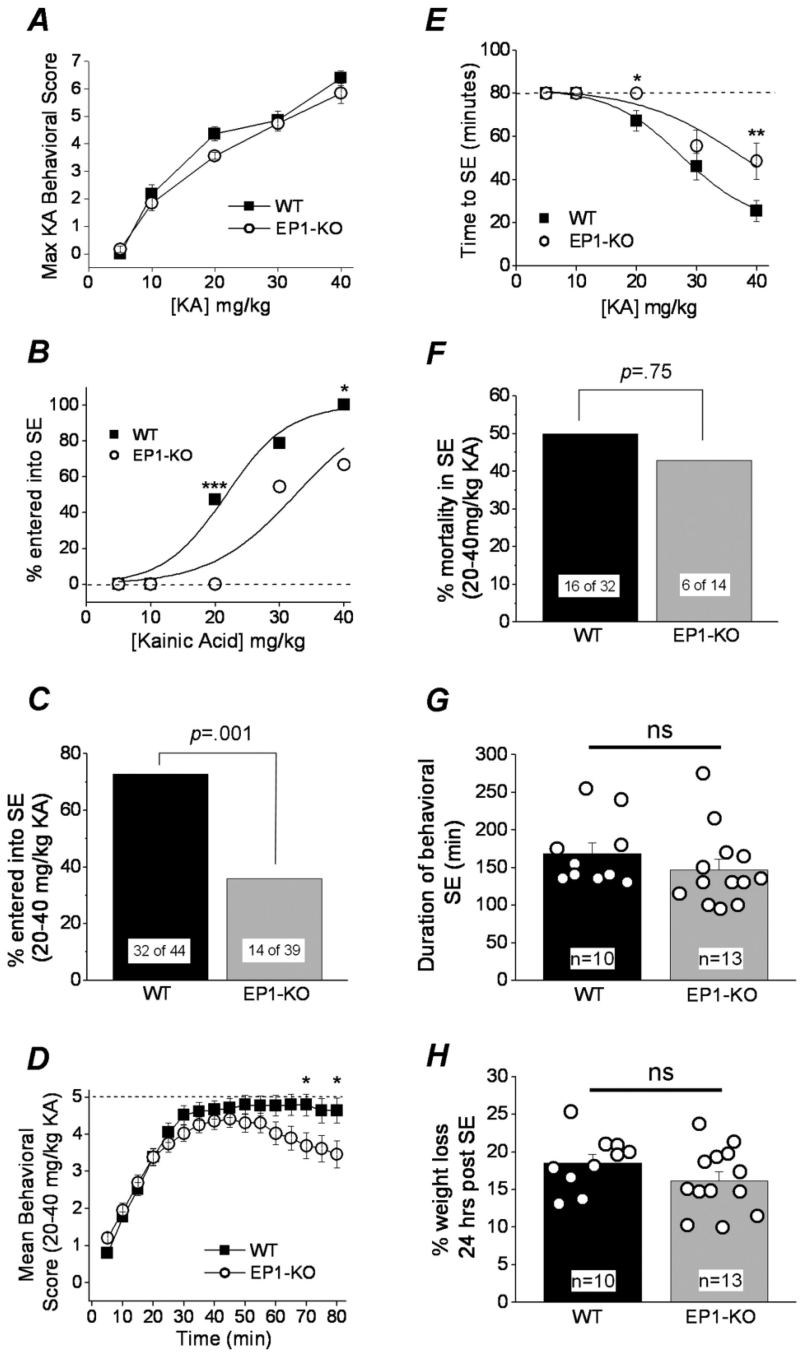

Figure 1. EP1 enhances kainate induced status epilepticus

A, a plot of the maximum behavioral seizure activity score over 80 min as a function of kainic acid concentration. Each point consists of a group of mice (wildtype or EP1-KO) injected s.c. with a single dose of kainic acid (wildtype, *n* = 12-17; EP1-KO, *n* = 11-16). ***B***, The kainic acid dose response curve for mice entering status epileptics (ED_{50} = 21.7 mg/kg wildtype, *n* = 12-17; ED_{50} = 32.4 mg/kg EP1-KO, *n* = 11-16). ***C***, comparison of the percent of mice that entered status epilepticus following injection with the intermediate and high kainic acid doses. ***D***, the mean behavioral score of all mice that received a single injection of

the intermediate and high concentrations of kainic acid (20, 30, 40 mg/kg) is plotted as a function of time. The temporal evolution of seizure activity suggests that both wildtype and EP1-KO mice progressed towards status epilepticus in a similar manner, but the behavioral seizure activity of the EP1-KO mice waned earlier than in wildtype mice (wildtype, $n = 44$; EP1-KO, $n = 39$). ***E***, the latency to status epilepticus onset following a single subcutaneous injection of intermediate and high kainic acid doses was different for wildtype and EP1-KO mice (wildtype, $n = 12\text{-}17$; EP1-KO, $n = 11\text{-}16$). The cutoff for status epilepticus onset was 80 minutes represented by the dashed line. Data points that are on the dashed line indicate groups of mice that failed to enter status epilepticus. ***F***, the percent mortality during status epilepticus was similar for both wildtype and EP1-KO. The total duration of behavioral status epilepticus (***G***) and the percent weight loss (***H***) 24 hours post status epilepticus following IP administration of a high kainic acid dose (30 mg/kg) was the same for wildtype (n=10) and EP1-KO mice (n=13), *t* test. The error bars indicate the standard error of the mean (SEM). WT, wildtype; SE, status epilepticus. One-way ANOVA with post hoc Bonferonni for group average in panels *A*, D, *and E*; Fisher's exact test was carried out for panels B, *C* and *F;* [* $p < .05$, ** $p < .01$, *** $p < .005$; $p > .05$ is considered not significant (ns)]. The error bars indicate the standard error of the mean (SEM). WT, wildtype; KA, kainic acid.

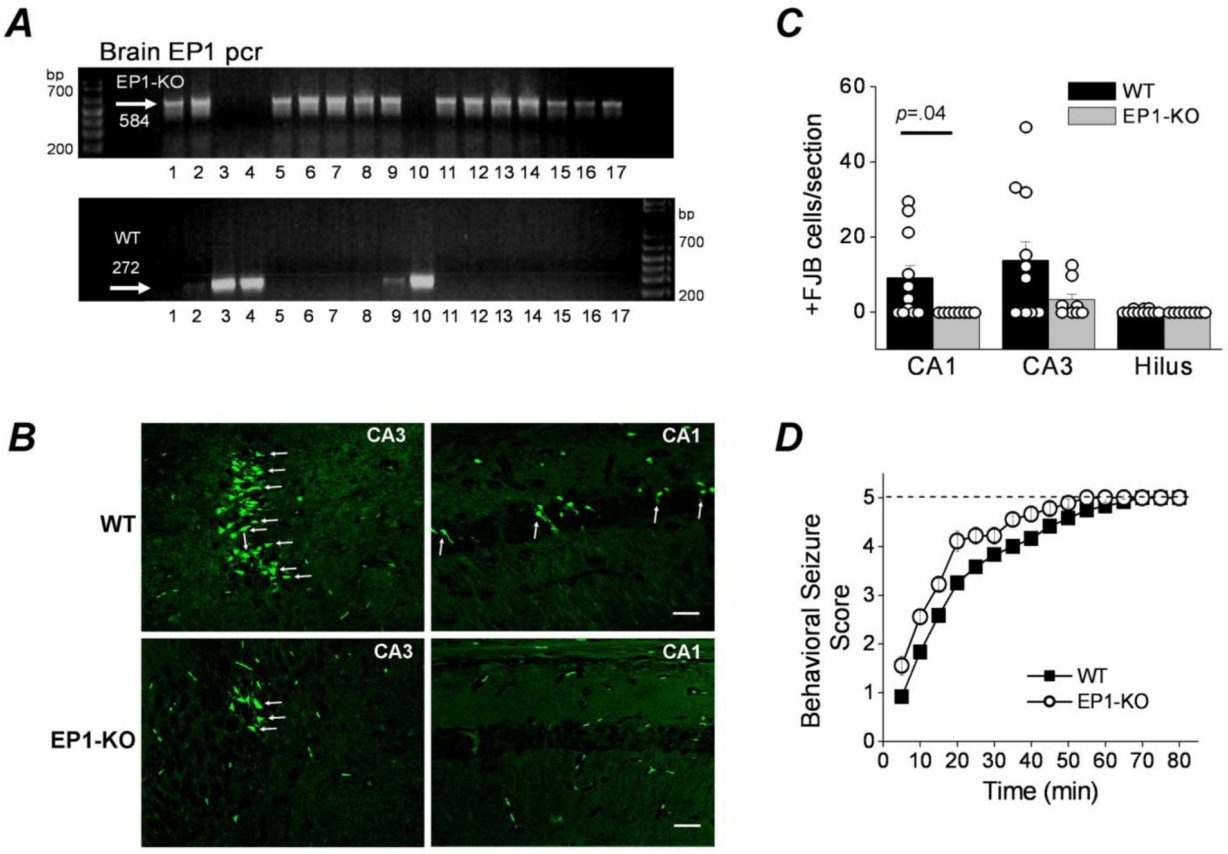

Figure 2. Neuroprotection in the EP1-KO following kainic acid induced status epilepticus

A,, digital image of a 1% agarose gel in which end point RT-PCR products from 17 mouse brain extracts were separated by size to identify amplicons of the targeted EP1 mutated gene in EP1-KO mice. The ladder is a 1kb plus DNA ladder. The horizontal arrows indicate the bands of interest. Vertical arrows indicate the 8 EP1-KO mice used for neurodegeneration counts in Panel C. ***B***, FluoroJade B staining in hippocampal sections (8 μm) revealed more injured neurons in the CA1 and CA3 layers for the wildtype compared to EP1-KO mice four days following status epilepticus (compare top to bottom panels). Images were taken at 100×. Scale bar, 50 μm. Arrows indicate representative FluoroJade B positive cells. ***C***, a plot of the number of FluoroJade B positive cells in hippocampal layers. Each open circle represents the average number of FluoroJade B positive cells per section in different mice; cells were counted in the hippocampal regions four days following kainic acid induced status epilepticus. The bars indicate the mean of each group. The number of wildtype (n = 11) and EP1-KO (n = 8) mice with FluoroJade B positive cells were compared with *t* tests. ***D***, the temporal evolution of seizure activity as judged by the behavioral seizure activity score (modified Racine scale) were similar for wildtype and EP1-KO mice that were used in this experiment (wildtype, *n* = 12; EP1-KO, *n* = 8). The dashed line indicates the behavioral score at the onset of status epilepticus. WT, wildtype; KA, kainic acid.

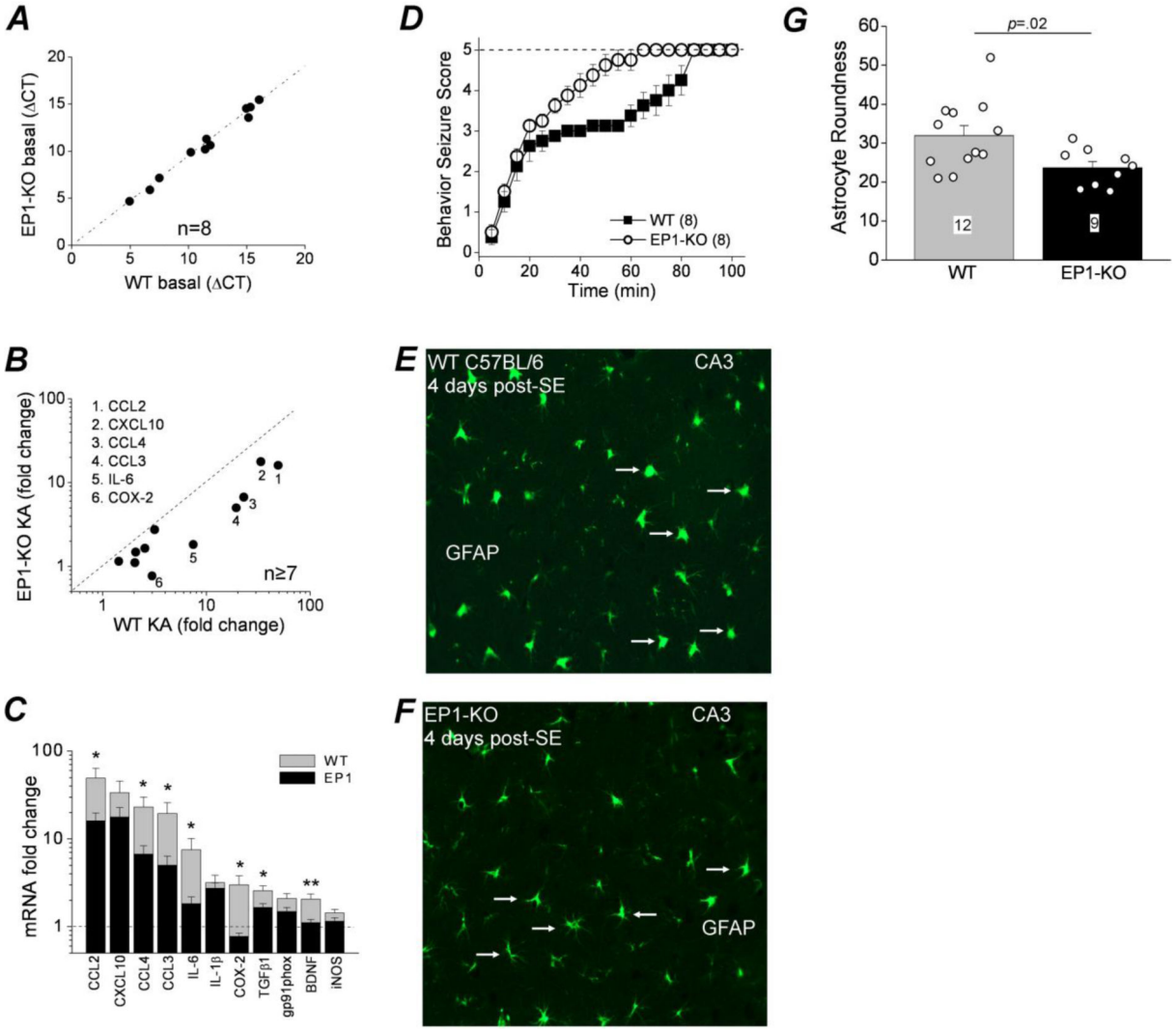

Figure 3. Induction of inflammatory mediators after status epilepticus is less robust in EP1 lacking mice

A, the basal levels of mRNA encoding inflammatory cytokines and mediators were similar in wildtype and EP1-KO mice injected with 0.9% saline. ***B***, induction of inflammatory mediator mRNA 24 hours following status epilepticus induced by i.p. injection of 20-40 mg/kg kainic acid. The inflammatory mediators were induced to different degrees in wildtype mice compared to EP1-KO mice. Transcripts that were most greatly blunted in the EP1-KO mice compared to wildtype following status epilepticus are represented by the numbers below the symbols. ***C***, the mean fold change ± standard error of all 11 inflammatory mediators is plotted for wildtype (n≥7) and EP1-KO mice (n=8) [* $p < .05$, ** $p < .01$, *t* test]. Data above the dashed line indicates an increase in mRNA levels. ***D***, the temporal evolution of seizure activity for mice used in this experiment (wildtype, $n = 8$; EP1-KO, $n = 8$). The EP1-KO mice reached status epilepticus faster than wildtype mice however all of the mice reached status epilepticus within 90 minutes. The dashed line indicates the behavioral score at the onset of status epilepticus***. E-F,*** Representative fluorescence images (200x total magnification) showing positive GFAP immunostaining

(green) as an astrocyte marker in the hippocampal CA3. Four days after status epilepticus, there was more astrogliosis as defined by the roundness of the cell bodies and shortened astrocyte processes in the sections taken from wildtype mice (n=12) (*E*) compared to sections taken from EP1-KO mice (n=9) (*F*). The arrows indicate typical astrocytes in each group. ***G***, the quantification of astrogliosis defined by the roundness of the cells measured in pixcavator IA 6.0. The average roundness of astrocytes from wildtype (n = 12) and EP1-KO (n = 9) mice were compared with a *t* test.

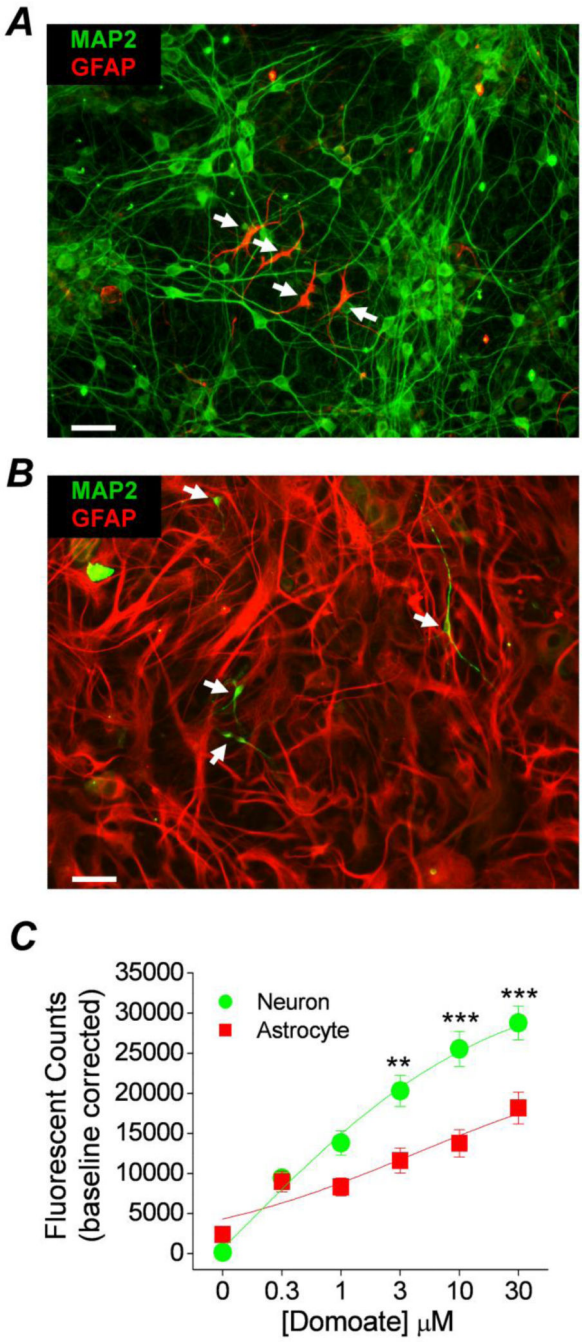

Figure 4. Purity of rat cortical cultures

Immunocytochemistry was performed on rat cortical cultures prepared to favor neuron growth ***A*** or astrocyte growth ***B***. Images were taken at 200x magnification using a high speed spinning disk confocal microscope. Positive fluorescent staining was observed for the neuron marker microtubule associated protein 2 (MAP2) and the astrocyte marker glial fibrillary acidic protein (GFAP) in both culture preparations. The confocal images show that neuron dense cultures contain far more MAP2 positive cells than GFAP positive cells. On the other hand astrocyte dense cultures contain far more GFAP positive cells than MAP2

positive cells. The scale bars are 20 μm. ***C***, the Ca^{2+} dependent fluorescent signal of rat neuronal dense and astrocyte dense cortical cultures loaded with Fluo-4 was monitored using the integrated fluidics of the FLEXstation. In neuronal cultures pretreated with AMPA, NMDA, and GABA receptor blockers a rise in fluorescence was measured 3 min after application of domoic acid (kainate receptor agonist). A plot of the intracellular calcium signal as a function of domoic acid concentration revealed a concentration-dependent relationship in both types of cultures. However, there is a difference in the intensity of the signal. Data are the mean ± standard error of the peak calcium signal of multiple experiments from three independent cultures (** $p < .01$, *** $p < .001$, one-way ANOVA with Bonferroni *post hoc* tests; domoate EC_{50} = 1.3 μM, n=18 for neuron cultures; EC_{50} = 4.3 μM, n=12 for astrocyte cultures).

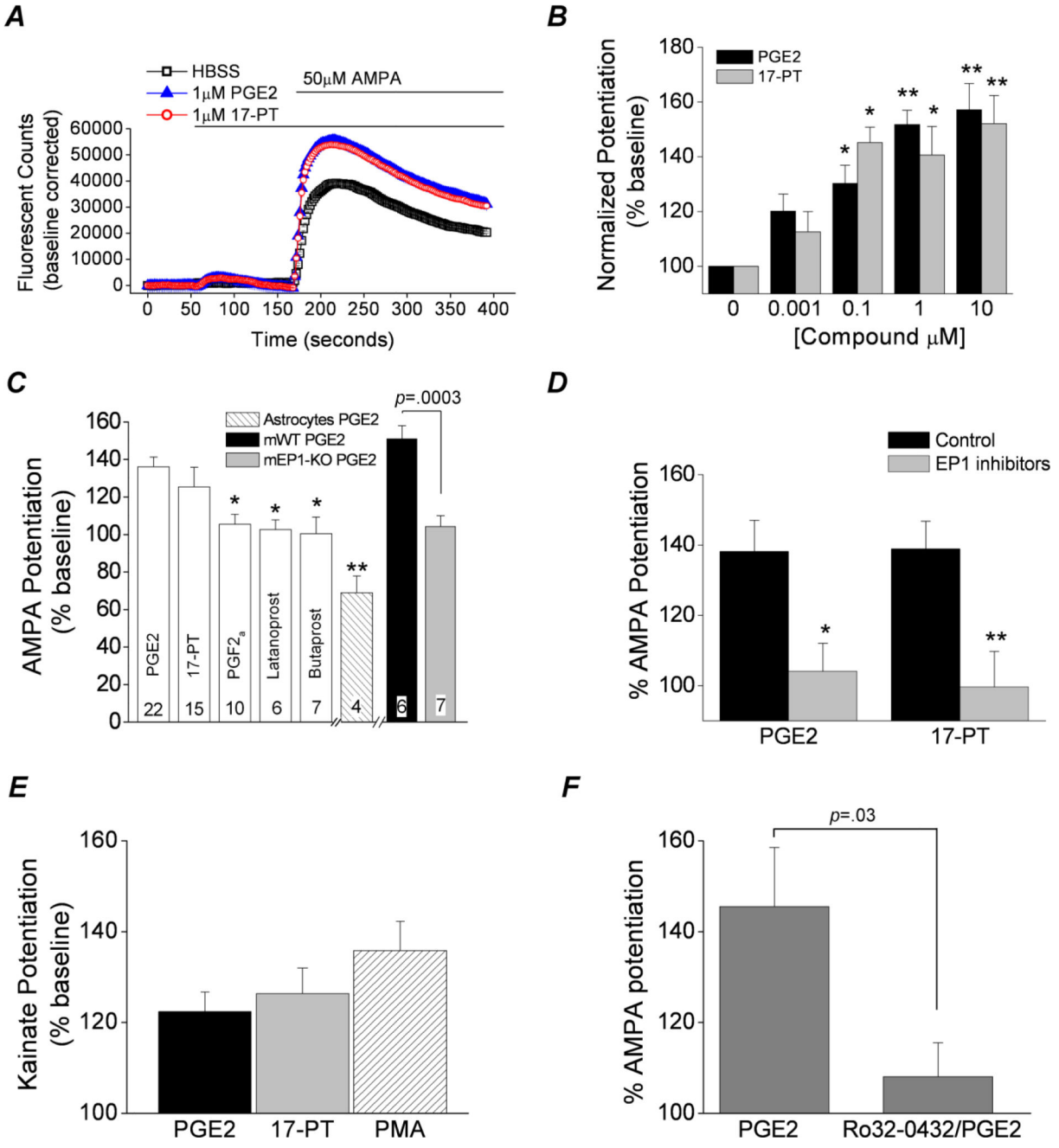

Figure 5. Activation of EP1 receptors potentiates kainate receptor Ca^{2+} signaling in mouse and rat cortical cultures

A, the Ca^{2+} dependent fluorescent signal of rat neuron cortical cultures pretreated with AMPA, NMDA, and GABA receptor blockers and loaded with Fluo-4 was monitored. Using the integrated fluidics of the FLEXstation II, a bolus of HBSS, PGE2 or 17-phenyl-trinor (17-PT) was delivered at 60 s following baseline stabilization, resulting in a miniscule change in the fluorescent signal. In rat neuron dense cortical cultures a rise in fluorescence was detected following application of AMPA (50 μM) at 180 s. The rise in intracellular Ca^{2+} upon AMPA exposure was potentiated by prior exposure to 1 μM PGE2 or 17-PT for 2

minutes. ***B***, the EP1 receptor induced potentiation of the AMPA mediated rise in the fluorescent counts was concentration-dependent in rat cortical cultures ($n \geq 6$; * $p < .05$, ** $p < .01$, one-way ANOVA with Dunnett's *post hoc* test). ***C***, the EP1 induced potentiation was not mimicked by the activation of other prostanoid receptors ($n \geq 6$; * $p < .05$ compared to potentiation by PGE2, one-way ANOVA with Dunnett's *post hoc* test). PGE2 (100 nM) potentiated the AMPA Ca^{2+} transient in cortical cultures from wildtype (mWT) (151 ± 7% of control) but not EP1-KO mice (mEP1-KO) (104 ± 6% of control). The PGE2 responses of the two mouse cultures were significantly different ($p < 0.05$, *t* test comparing mWT and mEP1-KO). PGE2 (10 μM) inhibited the response of rat astrocyte dense cultures to AMPA (69 ± 9% of control, n=4). The sample size is shown at the bottom of the bars. ***D***, a cocktail of EP1 receptor inhibitors (10 μM AH6809, 10 μM SC-51089 and 10 μM SC19220) eliminated potentiation of AMPA responses by both 100 nM PGE2 (138 ± 9% control vs 104 ± 8% with EP1 inhibitors, n = 10) and 100 nM 17-PT (139 ± 8% control vs 100 ± 10% with EP1 inhibitors, n = 10), * $p < .05$, ** $p < .01$, *t* test). Data for bars are the mean ± standard error. ***E***, the rise in intracellular Ca^{2+} upon kainic acid exposure was potentiated by prior exposure to 1 μM PGE2 (122 ± 4% of control, n = 13), 1 μM 17-PT (126 ± 6% of control, n = 13) and 100 nM PMA (a PKC activator) (136 ± 6% of control, n = 14) for 2 minutes. Data are the mean ± standard error. ***F***, a PKC inhibitor (Ro32-0432, 4 μM) strongly attenuated the kainic acid potentiation (AMPA in the presence of NMDA, AMPA and GABA receptor blockers) by 10 μM PGE2 (145 ± 13% control vs 108 ± 7% with PKC inhibitor, n = 6), $p = .03$, *t* test. Each symbol represents the AMPA potentiation of a single experiment, the bars are the mean of the group and the error bars are standard error of the mean.

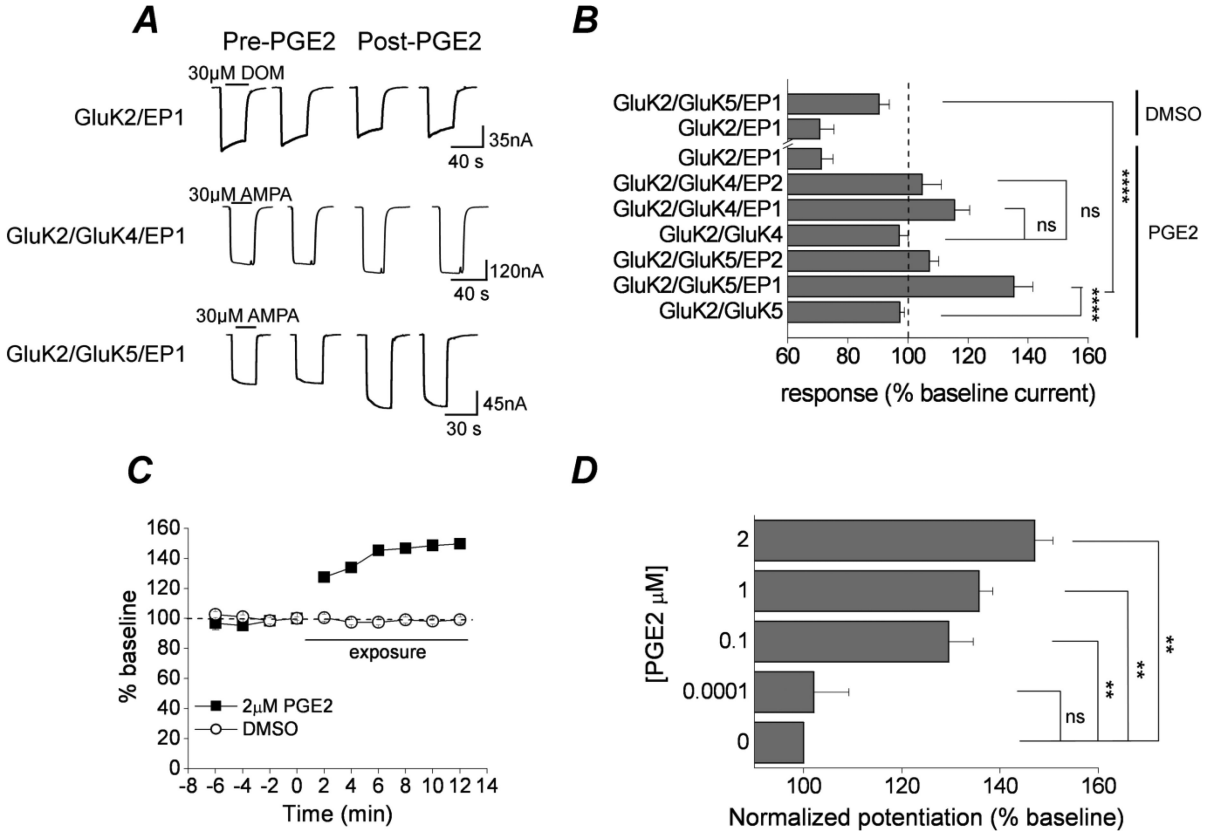

Figure 6. Potentiation of recombinant kainate receptors by EP1 prostanoid receptor activation

A, *w*hole-cell currents were recorded from oocytes 3 days after injection of GluK2/EP1, GluK2/GluK4/EP1, and GluK2/GluK5/EP1 RNAs. AMPA steady-state currents were potentiated following application of 2 μM PGE2 for the heteromeric, but not the homomeric kainate receptors. ***B***, Responses of different subunit combinations of the kainate and prostaglandin receptor RNAs. The largest potentiation was seen in oocytes expressing the GluK2/GluK5/EP1 (135 ± 6% of control, $n = 13$; **** $p < .001$, one-way ANOVA with Bonferroni *post hoc* test). Data are the mean ± standard error, n ≥ 5. $p > .05$ is considered not significant (ns). ***C***, time-dependent potentiation of GluK2/GluK5 AMPA currents by EP1 receptor activation (n = 6). ***D***, PGE2 concentration dependent response of GluK2/GluK5/EP1. Data are the mean ± standard error, n ≥ 4. $p > .05$ is considered not significant (ns), ** $p < .01$, n ≥ 5, one-way ANOVA with Bonferroni *post hoc* test).

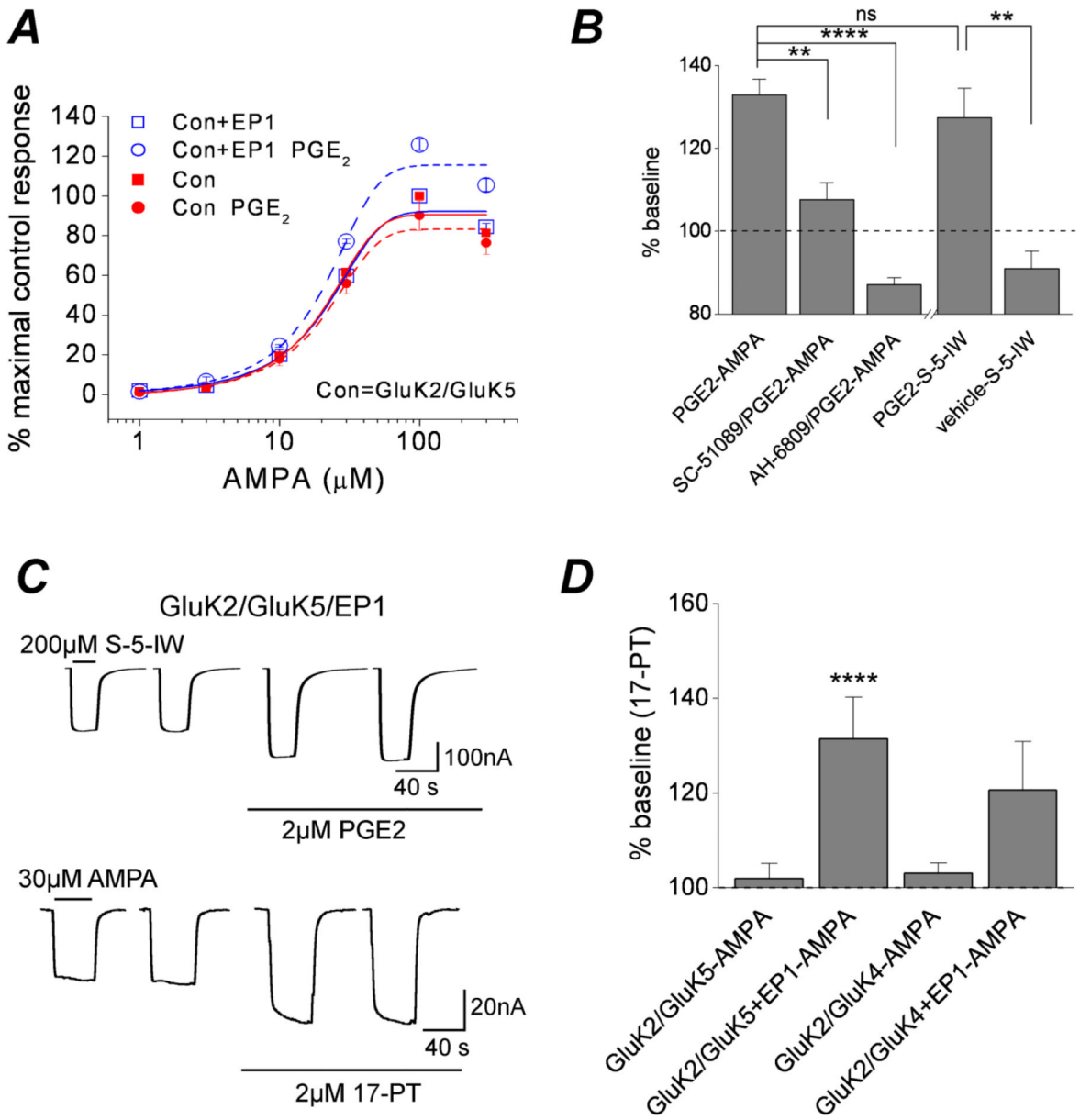

Figure 7. EP1 receptor activation is sufficient for kainate receptor potentiation

A, *w*hole-cell currents were recorded from oocytes 3 days after injection with the GluK2/GluK5 and GluK2/GluK5/EP1 RNAs. Exposure to increasing concentrations of AMPA elicited large inward currents that reached a steady-state. Shown are the mean and standard error of AMPA concentration-response curves from oocytes expressing GluK2/GluK5/EP1 and GluK2/GluK5 with or without prior exposure to 2 μM PGE2 (n ≥ 5). ***B***, the GluK2/GluK5/EP1 potentiation by 2 μM PGE2 (133 ± 4% of control, n = 21) was strongly attenuated or completely blocked in the presence of the EP1 antagonists SC-51089 and AH-6809 (108 ± 4% of control, n = 7 for SC-51089; 87 ± 2% of control, n = 11 for AH-6809; ** $p < .01$, **** $p < .001$, respectively; one-way ANOVA with dunnett's *post hoc* test). Exposure of oocytes expressing GluK2/GluK5/EP1 to S-5-iodowillardine (S-5-IW, a specific kainic acid agonist) elicited large inward currents that reached steady-state and

were augmented by exposure to 2 μM PGE2 (127 ± 7% of control, n = 12 for PGE2; 91 ± 4% of control, n = 5 for vehicle; ** $p < .01$, *t* test). The EP1 induced potentiation of steady state AMPA currents was not different from potentiation of steady state S-5-IW currents; one-way ANOVA with Dunnett's *post hoc* test. ***C***, Sample *w*hole-cell currents recorded from oocytes 3 days after injection of the GluK2/GluK5/EP1 RNAs. Steady-state S-5-IW currents were potentiated following application of 2 μM PGE2. Exposure of Xenopus oocytes expressing GluK2/GluK5/EP1 to 2 μM 17-PT potentiated AMPA induced GluK2/GluK5 currents in a similar manner as the natural agonist PGE2. ***D***, Exposure to 2 μM 17-PT potentiated GluK2/GluK5/EP1 (131 ± 9% of control, n = 5) and GluK2/GluK4/EP1 (121 ± 10% of control, n = 11), but had no effect on kainate receptor currents in the absence of the EP1 receptor (102 ± 3% of control, n = 20 for GluK2/GluK5; 103 ± 2% of control, n = 11 for GluK2/GluK4). Data are the mean ± standard error, **** $p < .001$; n≥5, one-way ANOVA with Bonferroni *post hoc* test.

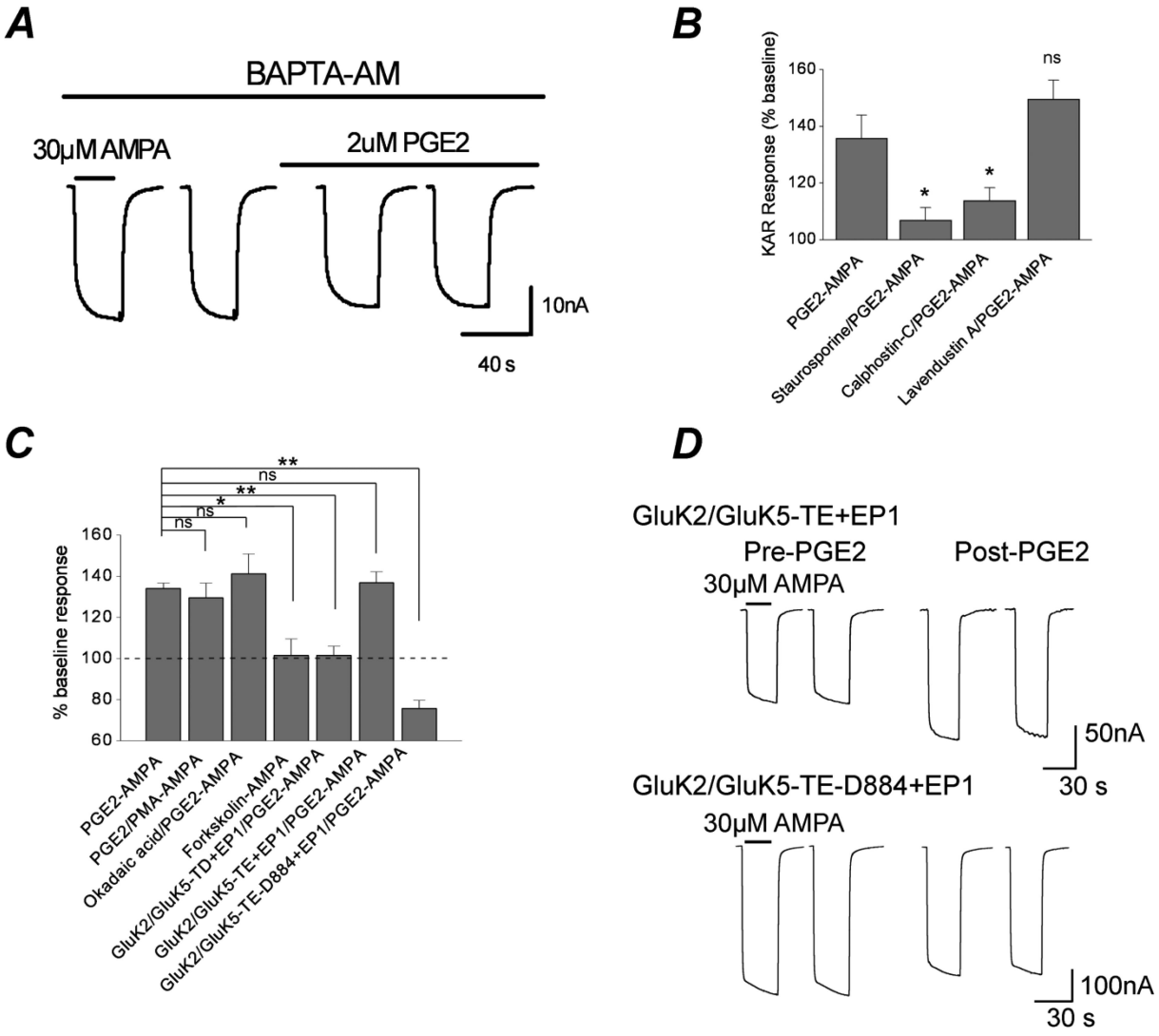

Figure 8. Dependence on PLC, Ca^{2+} and PKC

A, Sample recording from an oocyte expressing GluK2/GluK5/EP1 in the presence of BAPTA-AM prior to and following exposure to 2 μM PGE2. ***B***, staurosporine and the specific PKC inhibitor calphostin-C dramatically reduce PGE2-mediated potentiation of GluK2/GluK5/EP1 currents in oocytes. Pretreatment with the specific Src-tyrosine kinase inhibitor lavendustin A does not significantly alter PGE2 potentiation of kainate receptors. Data are the mean ± standard error, * $p < .05$, ** $p < .01$, $p > .05$ is considered not significant (ns); n ≥ 4, one-way ANOVA with Dunnett's *post hoc* test. ***C,*** Activation of PKC by PMA does not further potentiate the heteromeric GluK2/GluK5/EP1 beyond potentiation by PGE2 [134 ± 3% of control, n = 46 for PGE2 alone; 129 ± 7% of control, n = 9 for PGE2-PMA]. Okadaic acid (100 nM) treatment slightly enhances PGE2-induced potentiation of GluK2/GluK5/EP1 (141 ± 10% of control, n = 6). Forskolin (an indirect PKA activator) did not potentiate the GluK2/GluK5/EP1 (101 ± 8% of control, n = 4). Mutation of three serines (S833, S836, and S840) in GluK5 to aspartate (GluK5-TD) eliminated PGE2 sensitivity (101 ± 5% of control, n = 11). However, mutation of the same

three serines in GluK5 to glutamate (GluK5-TE) did not reduce PGE2 sensitivity (137 ± 5% of control, n = 12). EP1 activation depressed heteromeric kainate receptor currents when the three critical serines were mutated to glutamate and the C-terminus of GluK5 was truncated after amino acid 884 (GluK5-TE-D884) (76 ± 4% of control, n = 13). Data for bars are the mean ± standard error, * $p < .05$, ** $p < .01$, one-way ANOVA with Dunnett's *post hoc* test. ***D,*** The GluK5-S833E/S836E/S840 (GluK5-TE) mutant co-expressed with GluK2 and EP1 displayed a similar potentiation as the wildtype GluK2/GluK5+EP1 by PGE2. However, a mutant heteromeric receptor with the same three GluK5 serines mutated to glutamate combined with a C-terminal truncation after amino acid 884 (GluK2/GluK5-S833E/S836E/S840E-D884) showed no potentiation by PGE2 when co-expressed with EP1.

Table 1

CT values and geometric means of housekeeping genes in four groups of 8 mice for 24 hour inflammatory mediator measurement.

Genes:	WT basal	EP1-KO basal	WT KA	EP1-KO KA
HPRT1	21.7 ± 0.1	21.9 ± 0.1	21.6 ± 0.1	22.4 ± 0.4
β-ACTIN	17.2 ± 0.1	17.7 ± 0.1	17.0 ± 0.1	18.1 ± 0.5
GAPDH	16.2 ± 0.1	16.2 ± 0.1	16.1 ± 0.1	16.4 ± 0.3
Geomean	**18.2 ± 0.1**	**18.4 ± 0.3**	**18.1 ± 0.1**	**18.8 ± 0.3**

Data are the mean ± standard error

Table 2

Real Time PCR Primer Sequences

Genes:	Forward Primer (sequence 5'-3'):	Reverse Primer (sequence 5'-3'):
HPRT1	GGAGCGGTAGCACCTCCT	CTGGTTCATCATCGCTAATCAC
β-ACTIN	AAGGCCAACCGTGAAAAGAT	GTGGTACGACCAGAGGCATAC
GAPDH	TGTCCGTCGTGGATCTGAC	CCTGCTTCACCACCTTCTTG
CCL2	CATCCACGTGTTGGCTCA	GCTGCTGGTGATCCTCTTGTA
CCL3	TGCCCTTGCTGTTCTTCTCT	GTGGAATCTTCCGGCTGTAG
CCL4	CATGAAGCTCTGCGTGTCTG	GGAGGGTCAGAGCCCATT
CXCL10	GCTGCCGTCATTTTCTGC	TCTCACTGGCCCGTCATC
IL-1β	TGAGCACCTTCTTTTCCTTCA	TTGTCTAATGGGAACGTCACAC
IL-6	TCTAATTCATATCTTCAACCAAGAGG	TGGTCCTTAGCCACTCCTTC
iNOS	CCTGGAGACCCACACACTG	CCATGATGGTCACATTCTGC
COX-2	CTCCACCGCCACCACTAC	TGGATTGGAACAGCAAGGAT
gp91phox	TGCCACCAGTCTGAAACTCA	GCATCTGGGTCTCCAGCA
TGFβ1	ACTGCACCCACTTCCCAGT	TGTCCAGCTGGTCCTTTGTT
BDNF	GCCGCAAACATGTCTATGAGGGTT	TTGGCCTTTGGATACCGGGACTTT
GFAP	GACAACTTTGCACAGGACCTC	ATACGCAGCCAGGTTGTTCT
lba1	GGATTTGCAGGGAGGAAAAG	TGGGATCATCGAGGAATTG